# NATIONAL ADVISORY COMMITTEE FOR AERONAUTICS

REPORT 1276

# WIND-TUNNEL AND FLIGHT INVESTIGATIONS OF THE USE OF LEADING-EDGE AREA SUCTION FOR THE PURPOSE OF INCREASING THE MAXIMUM LIFT COEFFICIENT OF A 35° SWEPT-WING AIRPLANE

By CURT A. HOLZHAUSER and RICHARD S. BRAY


1956

For sale by the Superintendent of Documents, U. S. Government Printing Office, Washington 25, D. C. Yearly subscription, $10; foreign, $11.25; single copy price varies according to size - - - - - - - - - Price 25 cents

ERRATA

NACA Report 1276

By Curt A. Holzhauser and Richard S. Bray

Page 3, left column:

Change $\left(\frac{U_l}{U_{l_{max}}}\right)$ in the equation to $\left(\frac{U_l}{U}\right)_{max}$

Page 16, left column, right-hand portion of figure 22:

Ordinate values, $P_p$, should be negative.

NACA - Langley Field, Va.

Issued March 29, 1957

# REPORT 1276

## WIND-TUNNEL AND FLIGHT INVESTIGATIONS OF THE USE OF LEADING-EDGE AREA SUCTION FOR THE PURPOSE OF INCREASING THE MAXIMUM LIFT COEFFICIENT OF A 35° SWEPT-WING AIRPLANE

By CURT A. HOLZHAUSER and RICHARD S. BRAY

Ames Aeronautical Laboratory
Moffett Field, Calif.

# National Advisory Committee for Aeronautics

*Headquarters, 1512 H Street NW., Washington 25, D. C.*

Created by act of Congress approved March 3, 1915, for the supervision and direction of the scientific study of the problems of flight (U. S. Code, title 50, sec. 151). Its membership was increased from 12 to 15 by act approved March 2, 1929, and to 17 by act approved May 25, 1948. The members are appointed by the President, and serve as such without compensation.

# REPORT 1276

## WIND-TUNNEL AND FLIGHT INVESTIGATIONS OF THE USE OF LEADING-EDGE AREA SUCTION FOR THE PURPOSE OF INCREASING THE MAXIMUM LIFT COEFFICIENT OF A 35° SWEPT-WING AIRPLANE [1]

By Curt A. Holzhauser and Richard S. Bray


### SUMMARY

*An investigation was undertaken to determine the increase in maximum lift coefficient that could be obtained by applying area suction near the leading edge of a wing. This investigation was performed first with a 35° swept-wing model in the wind tunnel, and then with an operational 35° swept-wing airplane which was modified in accord with the wind-tunnel results.*

*The wind-tunnel and flight tests indicated that the maximum lift coefficient was increased more than 50 percent by the use of area suction. Good agreement was obtained in the comparison of the wind-tunnel results with those measured in flight.*


### INTRODUCTION

It has been observed in numerous investigations that the maximum lift coefficient of thin wings and wings with sweepback are frequently limited by air-flow separation from the leading edge of the wing. This type of air-flow separation is the result of large adverse pressure gradients developed over the forward portion of the airfoil at an angle of attack. The magnitude of these adverse pressure gradients can be reduced by the use of leading-edge camber or increased leading-edge radius, either of which tends to delay leading-edge air-flow separation to higher angles of attack, and consequently to higher values of lift coefficient. Another manner in which leading-edge separation can be delayed is to stabilize the boundary layer in the region of the leading edge so that these large adverse gradients can be tolerated. Two methods of stabilizing the boundary layer are to re-energize the boundary layer by blowing high-energy air into it, or to remove the low-energy portion of the boundary layer by means of suction.

A theoretical analysis made by Thwaites in 1946 (ref. 1) suggested that air-flow separation from the leading edge of an airfoil could be delayed by the use of only small quantities of suction air when distributed over a porous area. To distinguish this method of applying suction from that of suction through a slot, it is hereafter referred to as area suction. The two-dimensional experimental investigations reported in references 2 to 5 indicated that area suction could be applied at the leading edge of the airfoil to delay air-flow separation from the leading edge and that the suction flow quantities required were small. Because of the increases in maximum lift coefficient indicated to be possible with low suction flow quantities, a three-dimensional investigation was planned to obtain the information necessary for designing a porous leading edge for an airplane.

The three-dimensional investigation was to be performed in two phases; the first in the wind tunnel, and the second in flight. The purpose of the wind-tunnel test was to determine the effect of chordwise extent of porous area on the maximum lift coefficient as well as on suction requirements. These results were to be used to demonstrate the increases in maximum lift coefficient obtainable with area suction, and to make a comparison with the chordwise extents and suction flow quantities computed by the method set forth by Thwaites. The results were also to be used as a basis for the design of a porous leading edge and pumping system for the flight test vehicle. In additon to checking the wind-tunnel results, the purposes of the flight test were to evaluate and compare the flight characteristics of an airplane having leading-edge area suction with those of other high lift devices, namely a slatted leading edge and a leading edge modified to have increased camber and radius at the leading edge. The flight tests would also be used to ascertain the existence of possible limitations to the use of a porous leading-edge installation which could not be revealed by wind-tunnel tests.

In order to accomplish satisfactorily these objectives, an operational airplane was chosen as the basic vehicle for both the wind-tunnel and the flight investigations. This airplane was the F–86 which has a 35° swept-back wing and horizontal tail. The wing panels and horizontal tail of an F–86 airplane were modified and mounted on a research fuselage and tested in the Ames 40- by 80-foot wind tunnel in 1951. At the completion of the test, North American Aviation, Inc., received a contract from the United States Air Force to modify an F–86F airplane for the application of area suction at the leading edge of the wing. The design of the porous leading-edge installation was based on the wind-tunnel results. The airplane was then turned over to the NACA in 1954 for further instrumentation and flight testing. A standard F–86A airplane was used to obtain comparative flight characteristics of the airplane having a

[1] Supersedes NACA RM A52G17 by Curt A. Holzhauser and Robert K. Martin, 1952, and RM A55C07 by Richard S. Bray and Robert C. Innis, 1955.

normal leading edge, a slatted leading edge, and a leading edge having increased camber and radius. The results of the wind-tunnel and the flight tests are included in this report.

## NOTATION

$b$ wing span, ft

$c$ chord, measured parallel to the plane of symmetry, ft

$\bar{c}$ mean aerodynamic chord, $\dfrac{\int_0^{b/2} c^2 dy}{\int_0^{b/2} c\, dy}$, ft

$C_D$ drag coefficient, $\dfrac{\text{drag}}{qS}$

$c_l$ section lift coefficient, $(1/c)\oint P\, dx \cos\alpha - (1/c)\oint P\, dz \sin\alpha$

$C_L$ lift coefficient, $\dfrac{\text{lift}}{qS}$

$C_{L_{max}}$ maximum lift coefficient

$C_m$ pitching-moment coefficient, referred to quarter-chord line, $\dfrac{\text{pitching moment}}{qS\bar{c}}$

$C_Q$ flow coefficient, $\dfrac{Q}{US}$

$h_i$ total pressure at pump inlet, lb/sq ft

$l$ surface length of porous material, measured parallel to the plane of symmetry, ft

$H$ ratio of displacement thickness to momentum thickness of boundary layer, $\dfrac{\delta^*}{\theta}$

$p$ free-stream static pressure, lb/sq ft

$p_d$ static pressure in duct, lb/sq ft

$p_l$ local surface static pressure, lb/sq ft

$p_p$ static pressure in plenum chamber, lb/sq ft

$P$ airfoil pressure coefficient, $\dfrac{p_l - p}{q}$

$P_d$ duct pressure coefficient, $\dfrac{p_d - p}{q}$

$P_p$ pressure coefficient measured in plenum chamber of model or at pump inlet of airplane, $\dfrac{p_p - p}{q}$ or $\dfrac{h_i - p}{q}$, respectively

$q$ free-stream dynamic pressure, lb/sq ft

$Q$ volume of air removed through porous surface, based on free-stream density at test altitude, cu ft/sec

$R$ Reynolds number, $\dfrac{Uc}{\nu}$

$S$ wing area, sq ft

$t$ thickness of porous material, in.

$u$ velocity in the boundary layer, ft/sec

$U$ free-stream velocity, ft/sec

$U_l$ local velocity outside of the boundary layer, ft/sec

$U_{l_{max}}$ maximum local velocity outside of the boundary layer, ft/sec

$w$ suction-air velocity, normal to surface, ft/sec

$\dfrac{W}{S}$ wing loading of airplane, lb/sq ft

$x$ chordwise distance parallel to plane of symmetry, ft

$y$ spanwise distance perpendicular to plane of symmetry, ft

$z$ vertical distance, ft

$\alpha$ angle of attack referred to fuselage center line, deg

$\delta^*$ displacement thickness of boundary layer, ft

$\delta_f$ flap deflection, deg

$\Delta p$ pressure drop across porous material, lb/sq ft

$\eta$ fraction of semispan, $\dfrac{2y}{b}$

$\theta$ momentum thickness of boundary layer, ft

$\nu$ kinematic viscosity of air, sq ft/sec

## DESIGN OF THE POROUS LEADING EDGE

### PRINCIPLE OF AREA SUCTION—THWAITES ANALYSIS

The use of area suction to delay leading-edge type of air-flow separation was suggested by Thwaites in reference 1. This report presented a method by which the chordwise extent of porous area required to prevent leading-edge air-flow separation was estimated, and it presented equations whereby the suction quantities required for area suction and slot suction were calculated and compared. It was concluded in Thwaites' analysis that the application of area suction near the leading edge of an airfoil would delay leading-edge air-flow separation by the use of suction flow quantities only a small fraction of those required for suction through a slot.

It was reasoned by Thwaites that it is necessary to have porous suction extend chordwise on an airfoil only to the point where at the desired lift coefficient, the adverse velocity gradient is no more severe than the maximum velocity gradient reached prior to leading-edge air-flow separation without area suction. Since it is difficult to estimate the required chordwise extent of area suction by a comparison of velocity gradients, the simplifying assumption has been made that area suction is required in the region of the adverse velocity gradient where the ratio of local to free-stream velocity is greater than the maximum value reached without area suction. An example of this latter approximation is given in the following sketch. It has been found that the chordwise extents estimated by this simplified method are slightly greater than those estimated by a comparison of the pressure gradients.

In order to calculate the suction quantities required to delay leading-edge air-flow separation, use was made of the basic momentum equation for boundary-layer flow:

$$U\frac{dU}{dx}(\delta^*+2\theta)+U^2\frac{d\theta}{dx}=w(x)U+\nu\left(\frac{du}{dy}\right)_{y=0}$$

To simplify solution of this equation, Thwaites specified that the suction velocity, $w(x)$, be constant in the chordwise direction. He also specified that the velocity distribution through the boundary layer with suction applied would be maintained similar to that of a Blasius profile. With these simplifying specifications it was possible to find a chordwise distribution of velocity for which a Blasius boundary-layer profile could be supported with a given suction-air velocity.

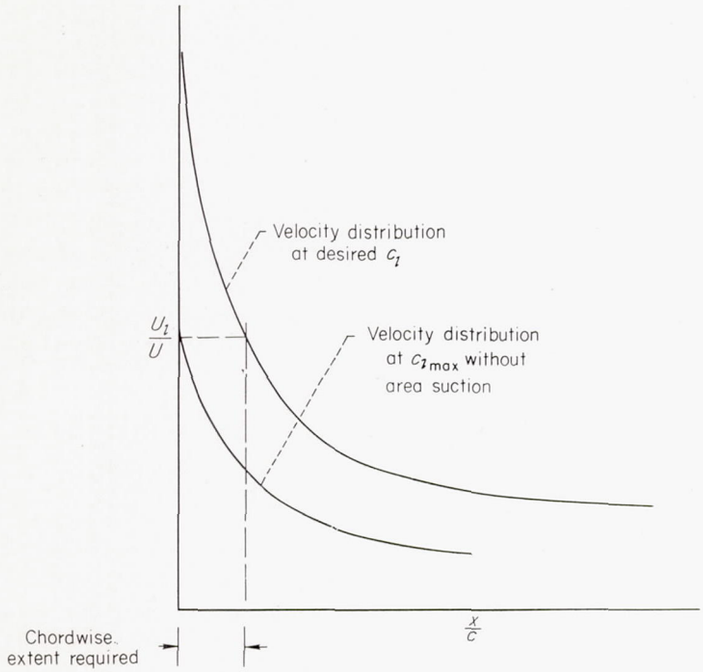


The suction-air velocity required at any desired lift coefficient could then be calculated from the equation:

$$\frac{w}{U}=\sqrt{K\left(\frac{U_l}{U_{l_{max}}}\right)\frac{1}{R}}$$

In this equation, $K$ is determined from a comparison of the chordwise velocity distribution of the airfoil at the desired lift coefficient with the chordwise velocity distribution which would support a Blasius profile with a particular suction-air velocity (ref. 1).

Since it was specified that the suction velocity be constant in the chordwise direction, and since the chordwise extent required was obtained previously, the suction quantity required for the desired lift coefficient of the airfoil section can be computed.

#### TWO-DIMENSIONAL APPLICATIONS OF AREA SUCTION

Several experimental investigations have been made with area suction near the leading edge of two-dimensional airfoils. The results of these tests are reported in references 2 to 5. These results indicated that applying area suction near the leading edge of the airfoil delayed air-flow separation and increased the maximum lift coefficient of the sections. In these tests, it was noted that the increases in the maximum lift coefficients obtained with area suction appeared to be limited by air-flow separation occurring either at the trailing edge of the airfoil or from the tunnel walls.

An application of Thwaites' analysis to the results of the tests reported in references 2 to 5 indicated that the method used to estimate the chordwise extent of porous area was valid. However, the suction quantities required for the two-dimensional tests were 10 to 15 times greater than the values computed by the equations derived by Thwaites. Further, for some lift coefficients, near the maximum values obtained with suction, the ratio of suction flow quantity to free-stream velocity had to be increased as the free-stream velocity was increased (refs. 4 and 5); whereas Thwaites' analysis indicated that this ratio should decrease.

At the present time, it cannot be determined to what extent the results of the two-dimensional tests were affected by the flow separation that occurred either at the trailing edge of the airfoil or from the tunnel walls.

#### THREE-DIMENSIONAL APPLICATION OF AREA SUCTION

An exploratory test performed on a 63° sweptback wing in the Ames 40- by 80-foot wind tunnel in 1949 showed that area suction was effective in delaying the leading-edge air-flow separation. When Thwaites' analysis was applied to the airfoil sections near the tip of this sweptback wing, the location of initial air-flow separation, the results were similar to those for two-dimensional sections in that the chordwise extents of porous area could be estimated but the suction-air velocities were about 10 times the values computed to be necessary. However, when Thwaites' analysis was applied to the sections inboard of the tip, it was found that the minimum chordwise extents found necessary for the tests were less than those estimated to be necessary; as on the wing tip, the minimum suction-air velocities used on the inboard sections were about 10 times the values computed to be necessary. The result that the chordwise extents of porous area inboard were less than the values indicated to be necessary is believed to be caused by a spanwise boundary-layer flow similar to that noted to exert a strong effect on the section maximum lift coefficients of the 45° swept wing of reference 6.

Although a lack of agreement existed between the theoretical and experimental results, it appeared that Thwaites' analysis could be modified to provide a first approximation in the design of the porous leading-edge installation. The manner in which this was done for the tests reported herein is described in the following paragraphs.

Tests were first performed on the 35° swept-wing model without boundary-layer control in order to obtain the force and pressure-distribution data for the basic model. A lift coefficient of 1.93 with flaps deflected was then chosen as the lift coefficient desired without air-flow separation, and a free-stream velocity of 112 feet per second was chosen for the test velocity. The section lift coefficients and the corresponding chordwise velocity distributions for four spanwise stations were then obtained for a wing lift coefficient of 1.93 by linear extrapolation of the measured data without area suction to an angle of attack corresponding to the wing lift coefficient of 1.93. This procedure was followed rather than the use of theoretical values or values obtained from two-dimensional tests because it was felt that linear extrapolation of the measured data provided more accurate values of the spanwise section lift variation and the chordwise and spanwise velocity distributions, particularly when the partial-span trailing-edge flap was deflected. The chordwise extents of porous area required at four spanwise stations were then obtained by a comparison of the individual velocity diagrams at section lifts corresponding to a wing lift coefficient of 1.93 with the comparable diagrams at the maximum section lift coefficients without area suction. The suction-air velocities at the same four spanwise stations were then computed for the desired wing lift coefficient of 1.93 and free-stream

velocity of 112 feet per second by using the equations set forth by Thwaites and the velocity diagrams at the desired section lift coefficient for each of the stations. The values of these requirements and the expected section lift coefficients are tabulated below:

| Spanwise station, $2y/b$ | Section lift coefficient, $c_l$ | Chordwise extent, $x/c$ | Ratio of suction-air to free-stream velocity, $w/U$ |
|---|---|---|---|
| 0. 25 | 1. 95 | 0. 027 | 0. 0030 |
| . 45 | 2. 11 | . 023 | . 0033 |
| . 65 | 1. 90 | . 020 | . 0040 |
| . 85 | 1. 76 | . 020 | . 0048 |

These values were then used in the design of the porous leading edge for the wind-tunnel model as follows. The chordwise extent of porous area was approximately doubled to allow ample freedom in adjusting the porous-area opening by trial and error. The suction-air velocities required were assumed to be 12 times the values computed (as an average between the factors of 10 to 15 noted in the previous tests). It was assumed that the suction-air velocities required to control separation should be constant in the chordwise direction. Since the external surface pressures vary in the chordwise direction whereas the internal duct pressure is constant, as shown in the following sketch, a porous material whose porosity varied along the chord was used to maintain

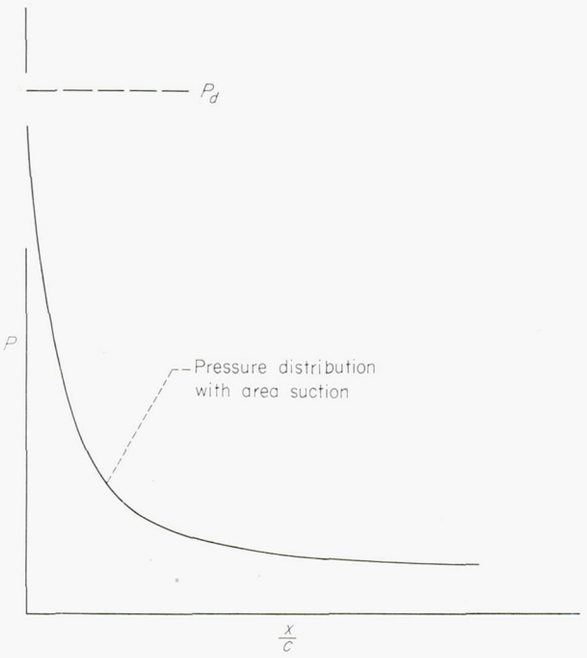


approximately constant suction-air velocities over the chordwise extent of porous area. It should be pointed out that Thwaites specified that the suction-air velocities be constant in the chordwise direction to simplify solution of the equations, and it is not known whether a constant suction-air velocity is necessary or even desirable for the lowest flow quantities.

The design of the porous leading edge of the flight vehicle, the F–86F airplane, was based on the results of the wind-tunnel tests of the 35° swept-wing model. The desired lift coefficient was 1.81 with flaps deflected and the free-stream velocity was 148 feet per second. It should be pointed out that the flight lift coefficient of 1.81 corresponds to an untrimmed lift coefficient of 1.93 measured in the wind-tunnel test. These values were chosen on the basis of the characteristics of the suction pump used and the wing loading of the airplane; further details may be found in reference 7. The suction-air velocities at the design condition were chosen as 16 times the values computed, in contrast to the factor of 12 used for the wind-tunnel investigation. The higher factor for the flight airplane was used to allow for the possibility of unknown adverse effects that might occur in flight. It was again specified that the suction-air velocities should be constant in the chordwise direction, and therefore the porous material used had a porosity that varied in the chordwise direction.

## DESCRIPTION OF RESEARCH VEHICLES, INSTRUMENTATION, AND TESTS

### WIND-TUNNEL MODEL

Since the wind-tunnel investigation was to be the basis of the design of an area-suction installation on an F–86 airplane, the wing panels and horizontal-tail surface of an F–86 were utilized on the model. These surfaces were mounted on a circular fuselage in the same relative location to each other as on an F–86 airplane. The general arrangement of this model is shown in the photograph of the model mounted in the tunnel, figure 1 (a), and in the two-view drawing, figure 2 (a). Additional dimensions of the model are provided in table I.

The wing had 35° of sweepback measured at the quarter-chord line and had an airfoil section of approximately 11 percent thickness normal to the quarter-chord line (coordinates of the airfoil are given in table II). The structure ahead of the front spar was replaced by the porous surface and ducting to enable application of area suction (figs. 3 (a) and 4 (a)). The porous surface near the leading edge of the wing consisted of an outer surface of metal mesh which was backed with a porous, hard wool felt material. The metal mesh had a thickness of 0.008 inch and had 11-percent open area (4225 square holes per square inch with each side of the hole about 0.005 inch long). This mesh extended from the 5-percent chord station on the upper surface to the 3-percent chord station on the lower surface of the wing, and from the intersection of the wing and fuselage ($2y/b=0.10$) to the beginning of the wing tip fairing ($2y/b=0.96$). The wool felt backing the mesh outer surface was tapered in the chordwise direction to provide the varying porosity required to compensate for the surface pressure distribution in order to obtain a constant suction-air velocity in the chordwise direction. The spanwise distribution of suction-air velocity specified for the design condition is shown in figure 5. The tapered wool felt was cut from ½-inch-thick material weighing about 9 pounds per square yard. This ½-inch-thick material had the pressure-drop variation with suction-air velocity shown in figure 6; for the range of suction-air velocities of interest, the pressure drop at a given suction-air velocity was proportional to the thickness of the felt. The thickness variations of the felt backing used in the wing are given in figure 7. It will be noted from this figure that while a continuously varying chordwise porosity was realized, the spanwise variation was made in four steps

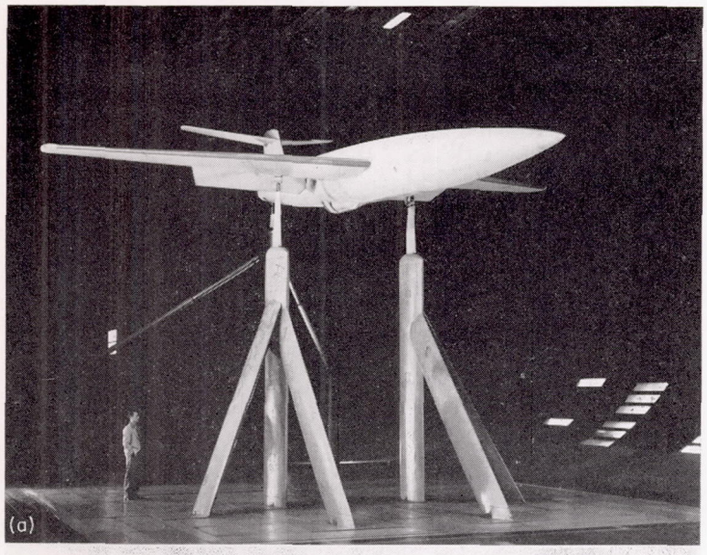


A-16742

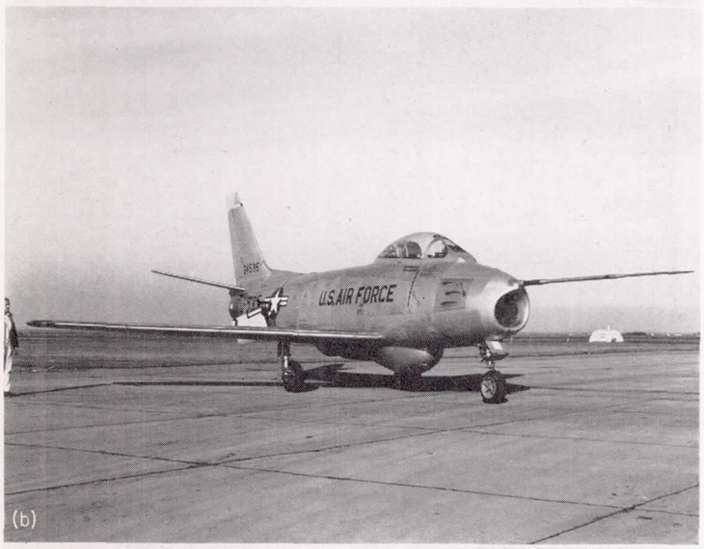


A-19919

(a) The 35° swept-wing model mounted in 40- by 80-foot wind tunnel.
(b) The F–86F airplane.

FIGURE 1.—Photos of the model and the airplane equipped with a porous leading-edge installation.

rather than continuously as specified in figure 5; this approximation was adopted since the specified variation was relatively small. Chordwise and spanwise extents of porous area were controlled by sealing with a nonporous cellulose tape 0.003 inch thick. In order to simulate the leading edge of an F–86 with slats retracted, the porous leading edge was completely taped. Partial taping of the porous leading edge provided the four spanwise distributions of chordwise extents studied in the wind-tunnel tests, configurations A, B, C, and D, shown in figure 8.

The normal F–86 ailerons and single-slotted flaps were retained on the model. The ailerons were locked in a neutral position, and the flaps were either undeflected or fully deflected, a deflection of 38° measured normal to the flap hinge line.

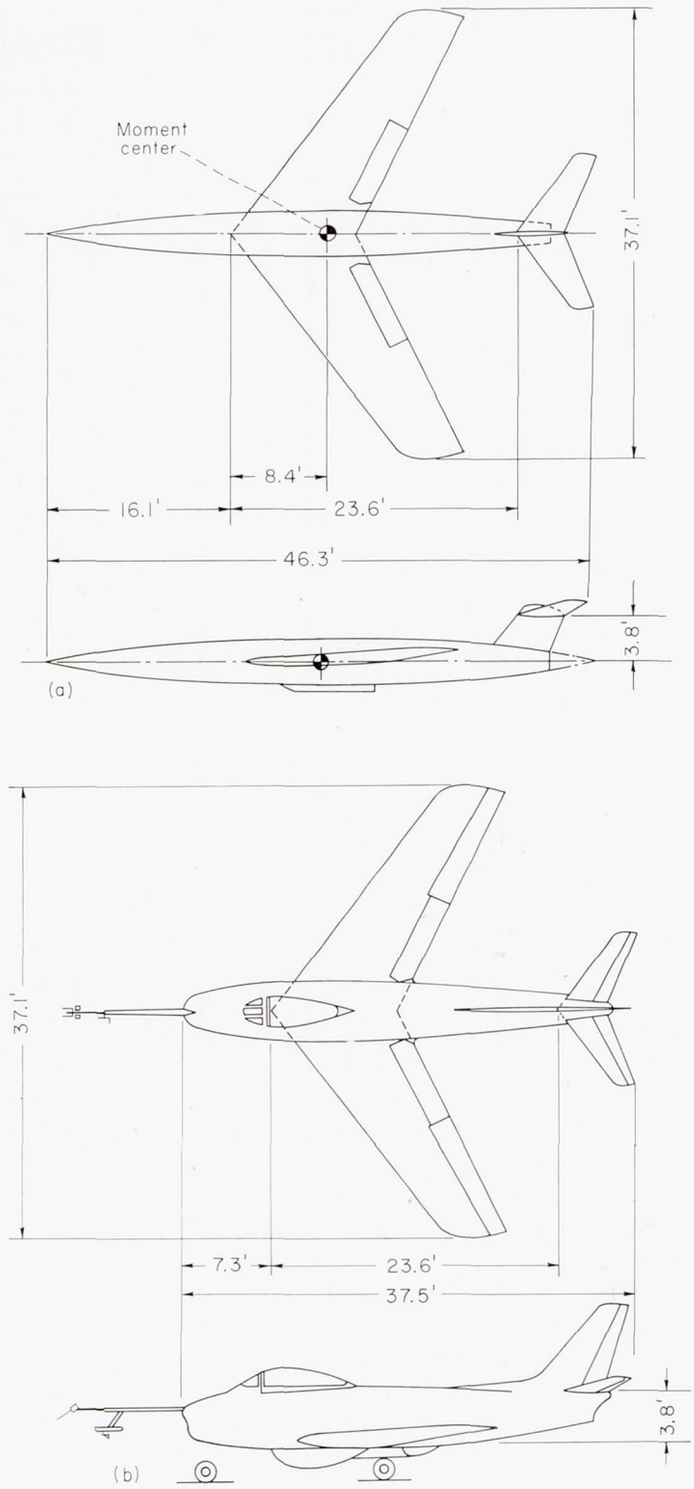


(a) The 35° swept-wing wind-tunnel model.
(b) The F–86F airplane.

FIGURE 2.—General arrangements of test vehicles equipped with porous leading-edge installations.

The fuselage used was circular in cross section and the radius, in feet, is defined by the equation $1.84\left[1-\left(\frac{x}{23}-1\right)^2\right]^{\frac{3}{4}}$. This fuselage has a larger fineness ratio (11.5 as compared to 6.9) and a smaller width (0.10 $b/2$ as compared to 0.13 $b/2$) than the fuselage of the F–86 airplane. Use of this

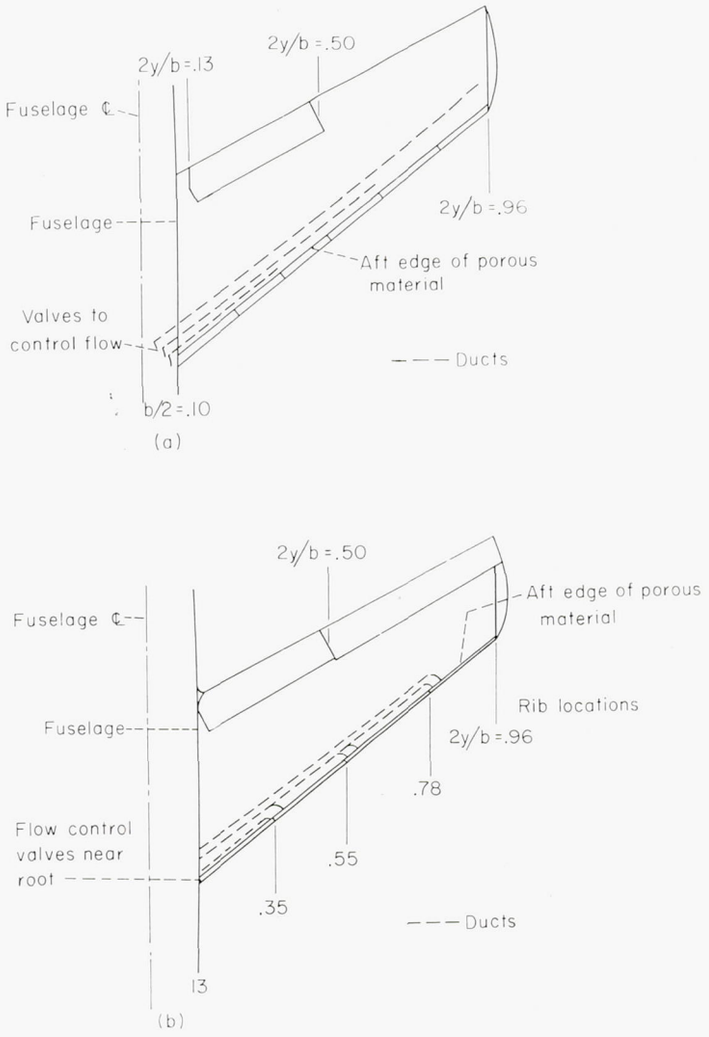


(a) The 35° swept-wing wind-tunnel model.
(b) The F–86F airplane.

FIGURE 3.—Plan view of wings with porous leading-edge installations.

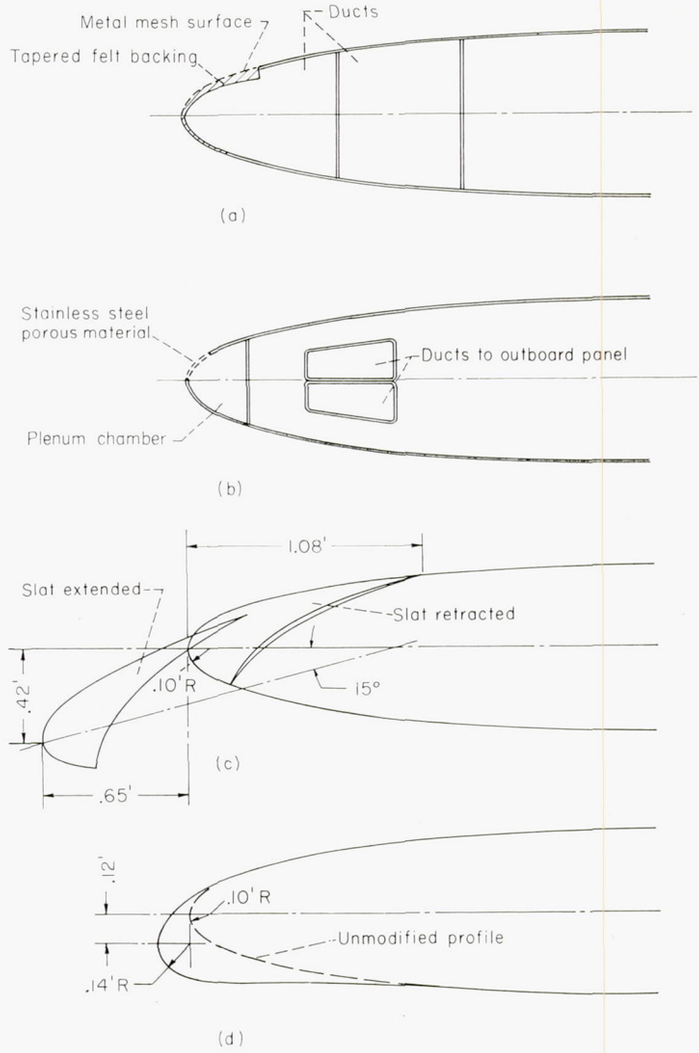


(a) Porous leading edge for wind-tunnel model.
(b) Porous leading edge for F–86F airplane.
(c) Slatted leading edge for F–86A airplane.
(d) Cambered leading edge for F–86A airplane.

FIGURE 4.—Cross sections of the various leading edges. Sections are normal to the quarter-chord line at the $0.47b/2$ station.

fuselage necessitated mounting the wings in a midwing location in contrast to the low wing position of the F–86 airplane.

The horizontal tail, which had 35° of sweep measured at the quarter chord line, was set at 0° incidence with the elevators set at 0° deflection.

The pumping equipment for the porous leading edge was housed in the fuselage. The pump consisted of the compressor portion of a turbosupercharger, and was driven by a 300-horsepower variable-speed electric motor. This pump induced the required suction flow quantities through the porous surface and then into ducts in the wing which had individual valves near the root of the wing to control the flow (see fig. 3 (a)). The air then dumped into a plenum chamber in the fuselage prior to entering the pump and was discharged from the pump through a duct in the bottom of the fuselage (see fig. 2 (a)). In order to measure the suction flow quantities, a survey rake was located at the exit on the bottom of the fuselage. This rake consisted of 54 total-pressure tubes, 9 static-pressure tubes, and 1 thermocouple and was calibrated against a standard ASME orifice meter. The power input to the suction pump was measured with a wattmeter.

To measure the external surface pressure distributions, static pressure orifices were installed on the upper and lower surfaces of the left wing in streamwise rows at $2y/b=0.25$, 0.45, 0.65, and 0.85; the chordwise locations of these orifices are given in table III. Orifices were also located in the ducts of the wing, as well as in the plenum chamber, in order to permit evaluation of the pumping requirements and duct losses.

### WIND-TUNNEL TESTS AND CORRECTIONS

Force measurements were made for all configurations throughout an angle-of-attack range of $-4°$ to 30°, at an angle of sideslip of 0°. The free-stream velocity was 112 feet per second which corresponded to a Reynolds number of $5.8\times10^6$ based on the mean aerodynamic chord. The spanwise distributions of chordwise extent of porous area, configurations A, B, C, and D, were obtained by trial and

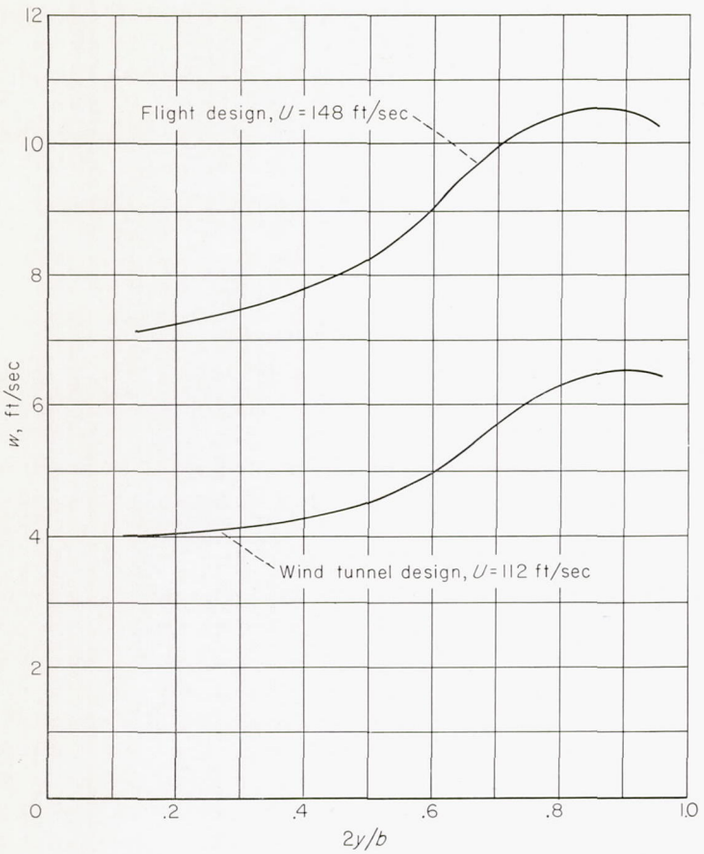


FIGURE 5.—Spanwise variation of the suction-air velocities desired for the porous-leading-edge installations.

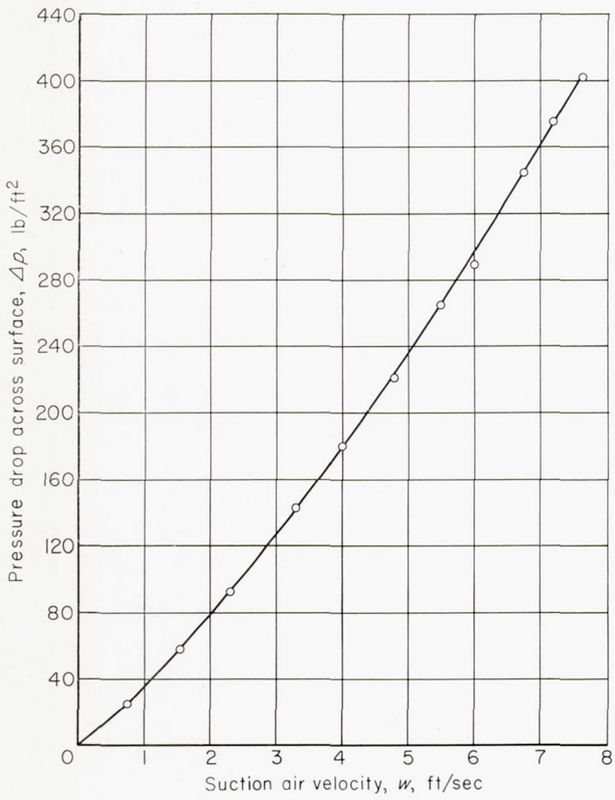


FIGURE 6.—Calibration of suction-air velocities for the porous mesh sheet backed with ½-inch wool felt.

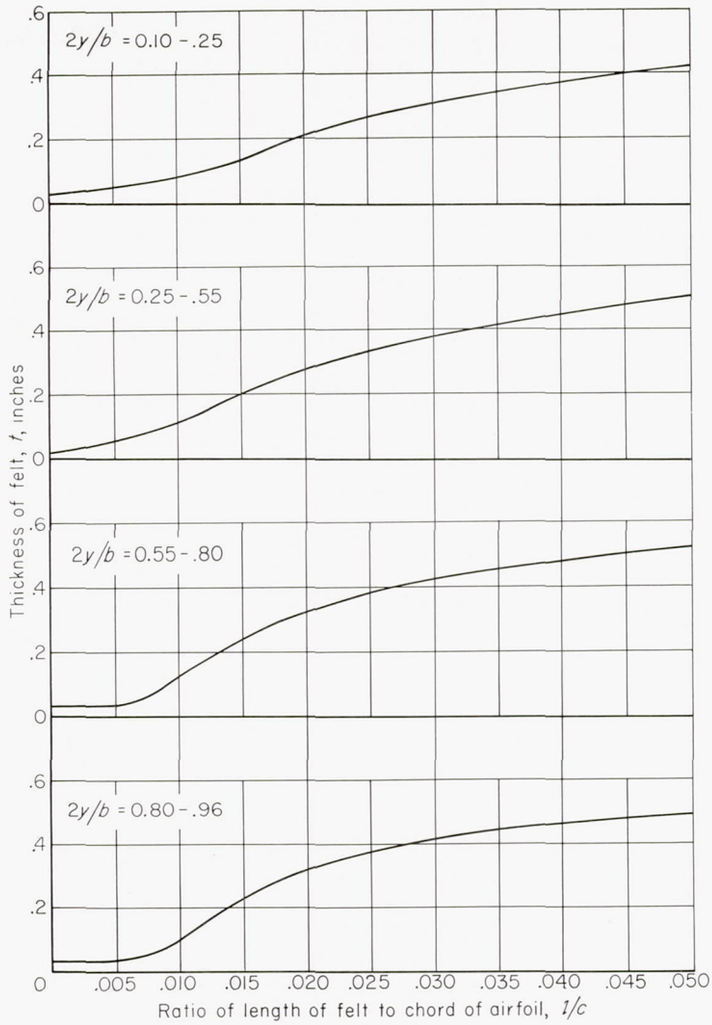


FIGURE 7.—Thickness variation of wool-felt backing used for porous leading edge of wind-tunnel model.

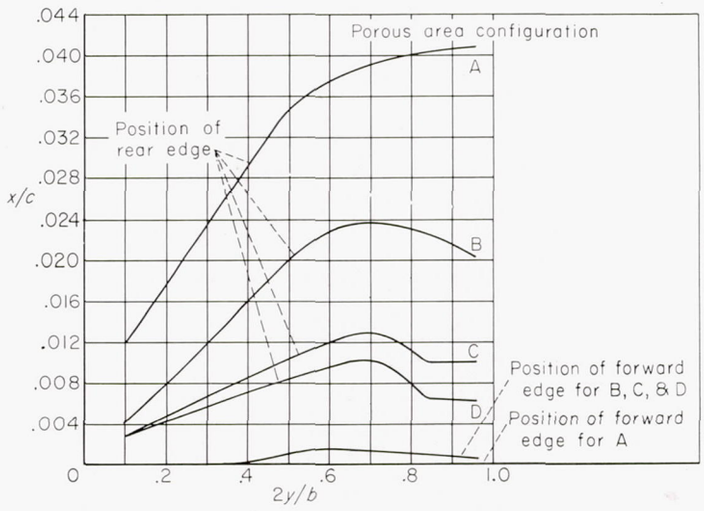


FIGURE 8.—The four spanwise distributions of the chordwise extents of porous area tested on the wind-tunnel model.

391603—57——2

error in the following manner: the lower surface of the porous leading edge was taped from the leading edge ($x/c=0$) to the rear edge of the porous surface ($x/c=0.03$); this area was taped for the entire test. Next, the upper surface was taped so that a constant width opening was obtained with the chordwise extent of porous area on the outboard portion of the wing approximating the value calculated to be necessary for the design lift coefficient of 1.93. For this configuration, a polar was run and the maximum lift coefficient and the flow coefficient required were measured. Then the rear edges of the inboard openings were progressively taped until a further reduction in chordwise extents would reduce the maximum lift coefficient. This procedure was repeated for the forward edge of the porus area and then for the tip of the wing. The resulting distribution of porous area was such that any further reduction in porous area extent anywhere along the span of the wing would result in a reduction in the maximum lift coefficient from the original value measured; this distribution of porous area was that of configuration B. A similar, although less extensive, procedure was followed in arriving at the distributions of porous area providing a higher maximum lift coefficient and two lower maximum lift coefficients. In order to determine the effects of free-stream velocity as well as to simulate the flow conditions of the F–86 airplane in a landing and a take-off configuration, additional measurements were made at free-stream velocities corresponding to wing loadings of 30, 40, and 50 pounds per square foot. These latter tests were made by changing the dynamic pressure of the wind tunnel for each angle of attack so that $C_L \times q$ was constant and equal to the wing loading, $W/S$. The maximum velocity at which these tests were performed was 180 feet per second which corresponded to a Reynolds number of $9.3 \times 10^6$. The various configurations and test conditions are summarized in table IV.

Standard tunnel-wall corrections for a straight wing of the same area and span as the sweptback wing were applied to the force data measured. No corrections were made for the strut interference, and no tares were applied to the pitching moment since they were believed to be negligible for the data of interest. Calculations indicated that the effect of the thrust of the exhausting air on the force characteristics was negligible.

The suction requirements (flow coefficients, duct and plenum chamber pressure coefficients, and power supplied to the blower) were measured for all configurations of the model with suction applied. However, only near the maximum lift coefficient were sufficient data taken with different values of suction flow coefficient to be able to define the minimum values of suction flow coefficient required to obtain the measured lift coefficient with the porous area installation tested. All values of flow coefficient presented were corrected to standard sea-level conditions. Limited measurements indicated that leakage resulting from the method of construction of the model was less than 10 percent of the total flow coefficient, and the values of flow coefficients were not corrected for this leakage. All values of the measured power input to the pump included pump losses and leakage. The duct losses were determined from pressure measurements in the duct behind the porous leading edge and in the plenum chamber just ahead of the compressor, and the pump losses were obtained from the characteristics of the pump. Consequently, the suction power required to compress the air from inside the wing ducts to a free-stream condition was then computed by subtracting from the measured power input the sum of the duct and pump losses.

Wool yarn tufts were taped to the upper surface of the wing during some of the tests to observe the boundary-layer flow characteristics as the stall was encountered.

### FLIGHT TEST AIRPLANES

**F–86F airplane with porous leading edge.**—The general arrangement of the F–86F airplane is shown in the photograph, figure 1 (b), and in the two-view-drawing, figure 2 (b). The airplane was a standard F–86F modified to incorporate a porous leading-edge installation. Dimensions of the airplane are given in table I.

The wing had 35° of sweepback at the quarter-chord line, and the structure forward of the front spar was modified to incorporate the porous leading edge and ducting in a manner similar to that of the wind-tunnel model (figs. 3 (b) and 4 (b)). However, the method of construction differed since it was desired to place no restriction on the operation of the airplane. The porous leading edge was constructed of panels of sintered, porous stainless steel having a constant thickness of about 0.050 inch, and having a varying porosity to provide a chordwise varying pressure drop in order to maintain the desired constant suction-air velocities over the chordwise extent at each spanwise station. The spanwise distribution of the suction-air velocity used for the design is shown in figure 5. Ground tests indicated that the pressure-drop characteristics of the leading-edge panels deviated locally from the design values a maximum of 30 percent. The spanwise distribution of the chordwise extent of the porous area used was that of configuration B (fig. 8), which was obtained by sealing portions of the porous leading edge with lacquer. The porous leading edge was stiffened by nose ribs only at the junctures of the porous panels. For each wing panel, these junctures, which are shown in figure 3 (b), formed four plenum chambers which were individually ducted to the vicinity of the wing root where they were joined in a single duct leading to the pump. Valves were located in each of the eight ducts to adjust the spanwise suction-flow distribution; these valves were closed to prevent flow through the pump and ducts when the pump was not being operated.

The pump used in this installation was a modified Thompson Products, Inc., B–31 turbosupercharger operated by high-pressure air bled from the compressor of the airplane's J–47 engine. The pump was mounted beneath the fuselage and was covered with a streamlined fairing (figs. 1 (b) and 2 (b)). A valve located in the bleed-air duct was adjusted by the pilot to control the pump speed. Due to limitations on the amount of air that could be taken from the engine, the maximum pump speed and resultant suction-flow quantity were dependent upon the engine speed. The suction-flow quantities were measured with a rake located at the pump inlet. This rake consisted of two total-pressure tubes

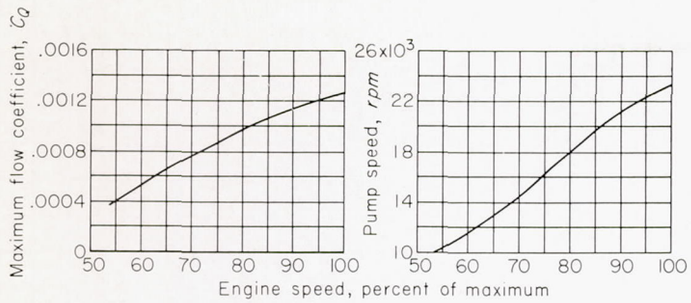


FIGURE 9.—Characteristics of the area-suction pumping system at the stalling speeds of the airplane; 7000 foot altitude.

and two static-pressure tubes and was calibrated against a standard ASME orifice meter. In figure 9 is shown the effect of engine speed on the maximum suction pump speed and on the maximum flow coefficient corresponding to conditions at the stalling speeds of the airplane at an altitude of 7,000 feet.

**F–86A airplane.**—The general arrangement and dimensions of the F–86A airplane were the same as the F–86F, except no pump and pod existed on the bottom of the fuselage. The F–86A was equipped with leading-edge slats which are shown in figure 4 (c). These slats could be locked in the retracted position or they could be allowed to extend automatically.

By removing the forward portion of the wing, the slatted leading edge was replaced with the cambered leading edge shown in figure 4 (d). This cambered leading edge also incorporated an increased leading-edge radius. The coordinates of this cambered leading edge are given in table II.

### FLIGHT TESTS AND CORRECTIONS

**F–86F airplane with porous leading edge.**—Measurements of the low-speed characteristics of the test airplane were taken at an altitude of 7,000 feet to permit complete stalling of the airplane without undue hazard. The data included in this report were taken from time-history records obtained in the following manner: with engine power and pump speed set at appropriate constant values, and starting at an airspeed above the suction-off stall speed, the nose of the airplane was slowly elevated in such a manner as to decelerate at a rate not exceeding 1 knot per second. The records were terminated when the pilot felt that the airplane was no longer controllable. The majority of these stalls were performed at 85-percent engine rpm in the interest of consistency in evaluating the stalling characteristics of the airplane. However, since the maximum flow coefficient obtainable at 85-percent engine rpm was about 0.0011, it was necessary to perform several stalls at 100-percent engine rpm to determine the lift characteristics of the porous leading edge with the maximum available flow coefficient of 0.0012. These flight tests were performed with the trailing-edge flaps undeflected as well as deflected 38°. The chordwise extent of the porous area on the leading edge of the airplane for all of the flights was that of configuration B (fig. 8). In addition to the tests with suction applied, tests were also made with suction off and the duct valves closed. During some of the tests, wool yarn tufts were taped to the upper surface of the wing; the behavior of the tufts at the stall was recorded photographically.

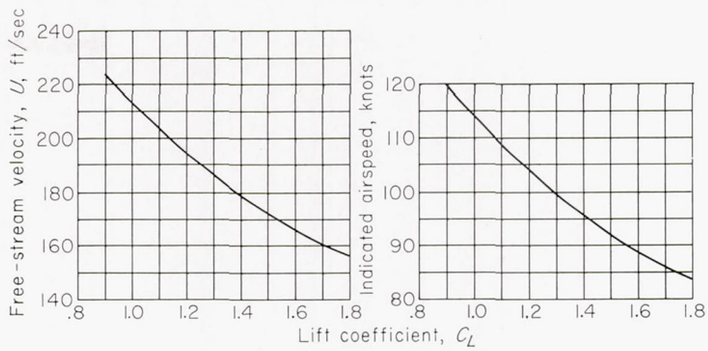


FIGURE 10.—Variation of free-stream velocity and indicated airspeed with lift coefficient for the conditions of the flight tests; 7000 foot altitude.

The variations of the indicated airspeed and free-stream velocities with lift coefficients for the average conditions of the tests are shown in figure 10. These relationships correspond to an average wing loading of about 45 pounds per square foot. The values of lift coefficients presented in this report are values corrected for the effect of the engine thrust; the values of engine thrust used were obtained from data provided by the manufacturer of the J–47 engine.

The flow coefficients measured were corrected to the static conditions at the test altitude. Limited measurements indicated that a negligible amount of leakage resulted from the method of construction of the porous leading-edge installation.

In addition to the quantititive tests previously mentioned, several qualititive tests were made with the airplane. These tests included evaluation of the landing and take-off performance as affected by the suction equipment. Several flights were also made in which the airplane was flown up to a Mach number of 0.9 and up to an altitude of 35,000 feet. These flights were conducted with the F–86F airplane with the porous leading edge and with a standard leading edge, in order to obtain comparative values with the pump installed and operating. Maximum speed and buffet characteristics were of primary interest in this phase of the investigation.

**F–86A airplane.**—Measurements of the low-speed characteristics of this test airplane were also taken at 7,000 feet, and the data presented in the report were obtained and corrected in the same manner as those for the F–86F airplane. These data were obtained with the slatted leading edge automatically extended, as well as locked in the retracted position. Similar data were also obtained for the airplane with the cambered leading edge.

The wing loadings of the F–86A were approximately the same as for the F–86F, and therefore the flight speed variation with lift coefficient presented in figure 10 is also applicable for the F–86A.

## RESULTS AND DISCUSSION

### WIND-TUNNEL TESTS

**Static longitudinal characteristics of model without suction applied.**—The three-component force data of the 35° sweptback wing model without suction are shown in figure 11 with the trailing-edge flaps fully deflected (38°) and undeflected

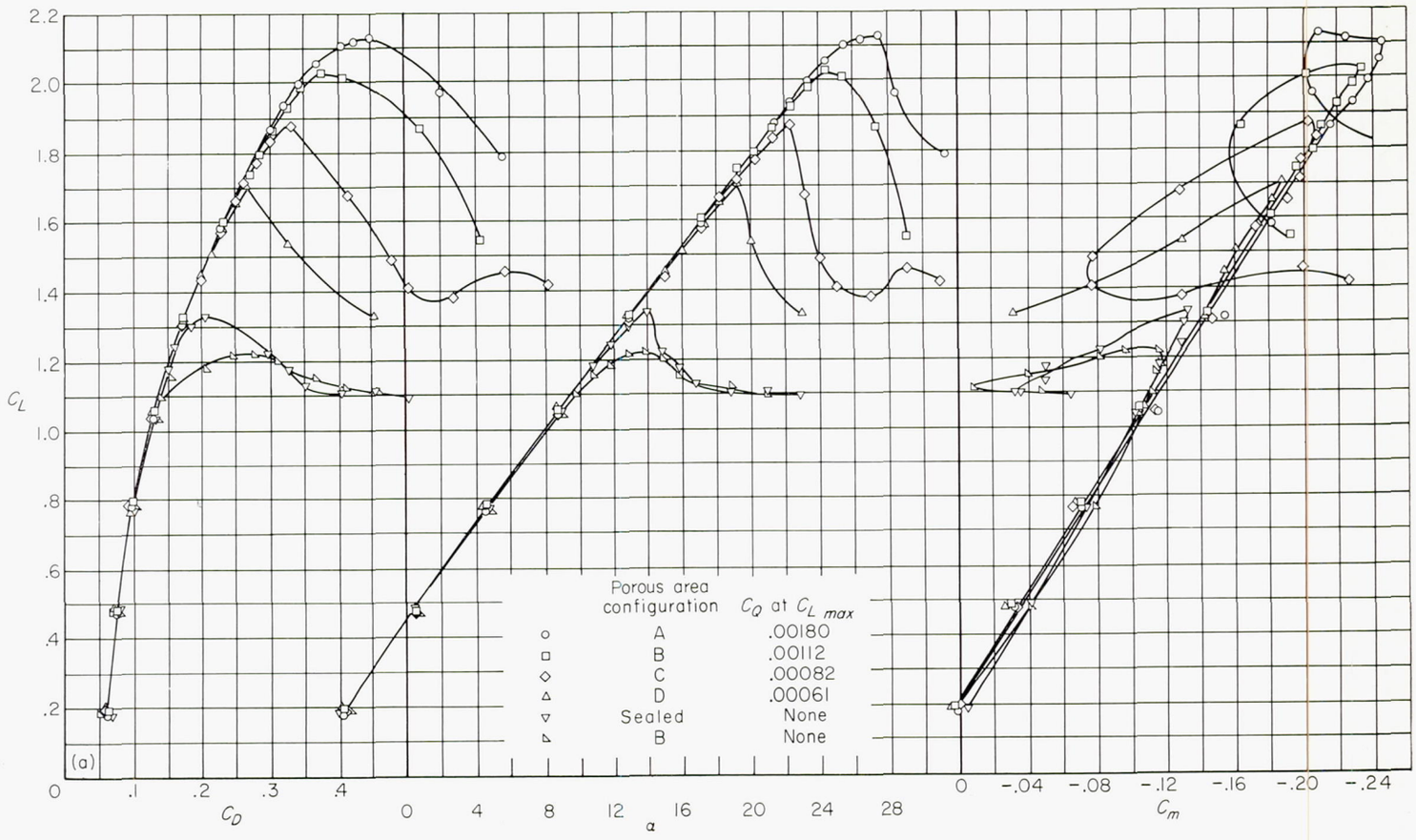


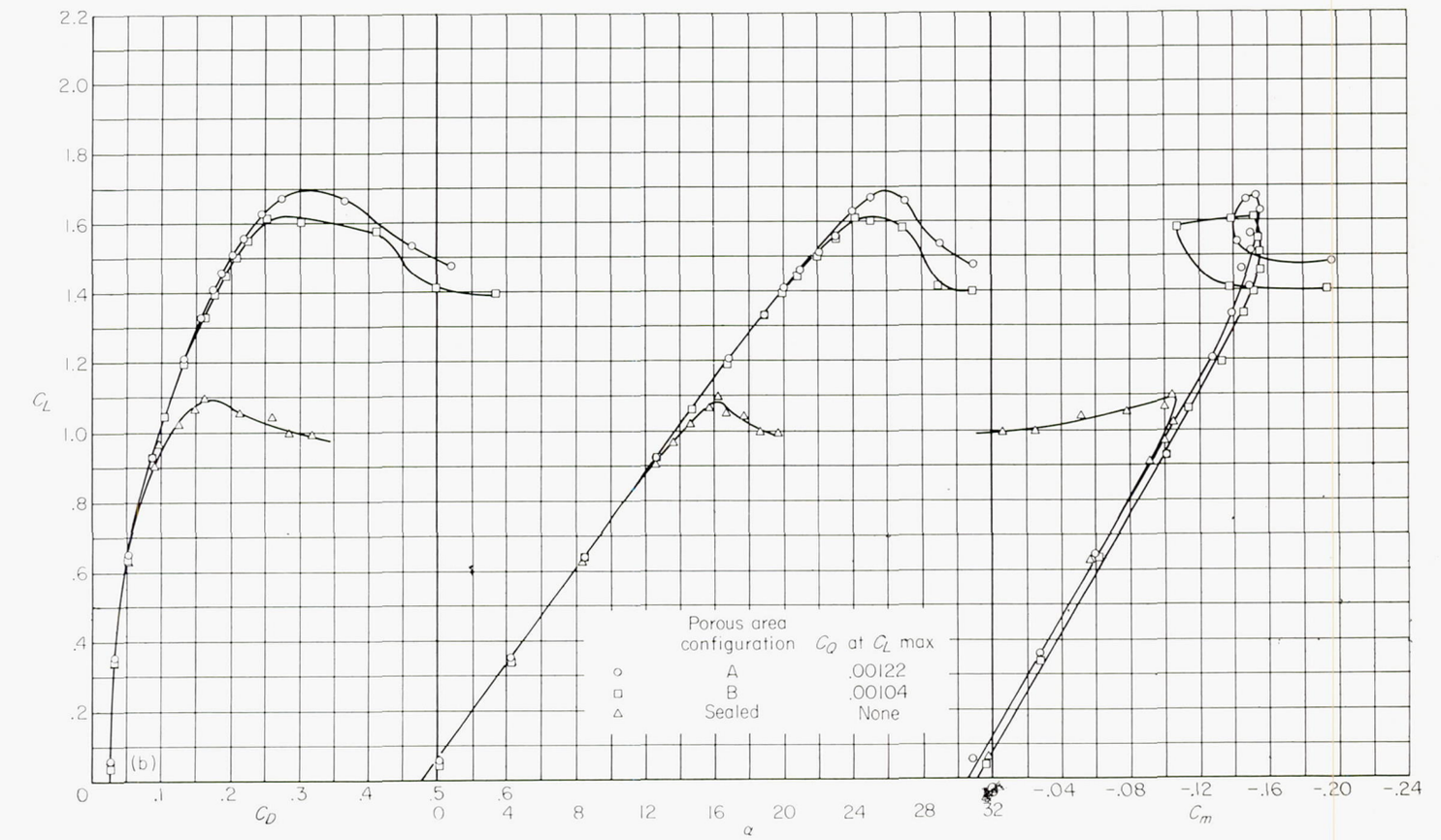


(a) $\delta_F = 38°$

(b) $\delta_F = 0$

FIGURE 11.—Aerodynamic characteristics of 35° swept-wing model with several chordwise extents of porous area; $U = 112$ feet per second.

(0°). The force characteristics with the porous leading edge sealed simulate the operational airplane with the slats closed. Also shown in figure 11(a) are the force characteristics for the model with the porous area open but with no suction, simulating the condition that would exist for the porous leading-edge installation when the suction pump is inoperative. The data of this figure show that the air circulating through the porous surface had a detrimental effect on the maximum lift coefficient of the model.

**Static longitudinal characteristics of model with area suction.**—Three-component force data of the 35° swept-wing model with several chordwise extents of area suction along the full span of the leading edge are shown in figure 11. Included in the figure are the values of flow coefficients required at the maximum lift coefficients for the different chordwise extents of area suction. The extensions of the linear portion of the lift and pitching-moment curves and of the drag parabola indicate that the use of area suction at the leading edge delayed air-flow separation. External surface pressure distributions with and without suction applied at 13° and 17° angle of attack are shown in figure 12. These distributions show that the pressure distributions were not changed when suction was applied at an angle of attack below that at which separation occurred without suction; whereas at larger angles of attack, the pressure distributions were changed from distributions indicating separation to ones indicating that the separation was eliminated by area suction. The effectiveness of area suction in delaying air-flow separation and, hence, increasing the lift coefficient of the wing is more clearly shown in figure 13 in which the section lift coefficients, obtained from integration of pressure distributions, are plotted as a function of angle of attack. The complete pressure distributions presented in graphical form at the end of this report (figs. 24 and 25) show the spanwise progression of the air-flow separation. The pressure distributions presented with suction applied are for the porous-area configuration B with flaps deflected; however, the effects of area suction on the pressure distributions were similar for the other configurations tested. The force and pressure data presented in figures 11, 12, 24, and 25 were for a free-stream velocity of 112 feet per second; however, it was found that increasing the free-stream velocity to 180 feet per second (the maximum velocity of the test) did not significantly alter these characteristics.

**Suction requirements of porous leading edge.**—In figure 11 values of flow coefficient required at the maximum lift coefficients measured with the different porous-area configurations are listed. These values of flow coefficient are indicative of the lowest values of flow coefficient which could be used for each of the openings tested and yet maintain the values of maximum lift coefficients shown in figure 11. For each of the configurations, a reduction in the maximum lift coefficient was measured when the flow coefficient was somewhat reduced; whereas, in contrast, doubling the flow coefficient from the values presented had a negligible effect on the maximum lift coefficient or on the angle of attack for the maximum lift coefficient. Thus, it is seen that the angle of attack and the maximum lift coefficient to which the air-flow separation could be delayed were determined

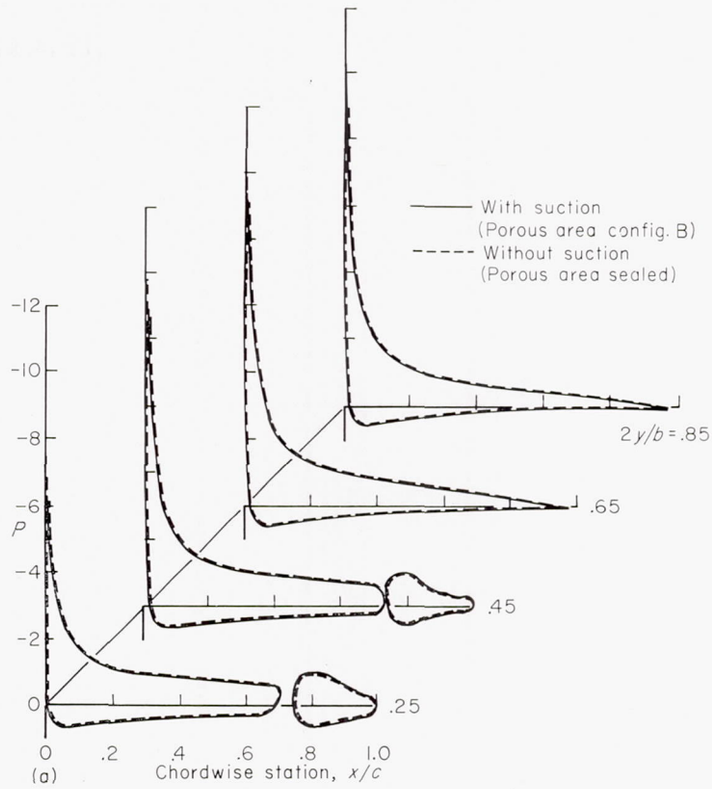


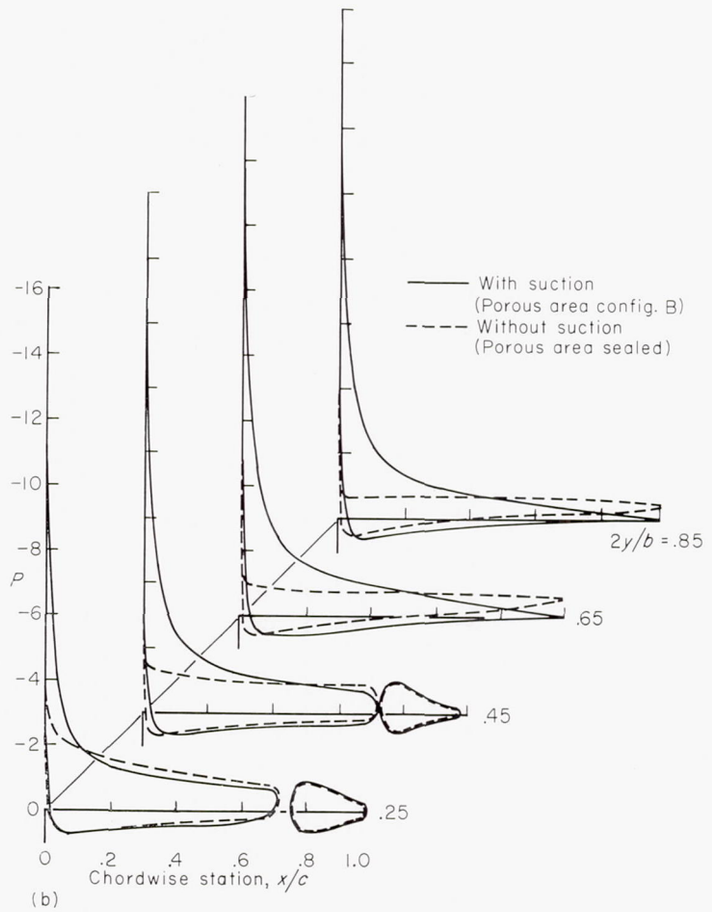


(a) $\alpha = 13°$
(b) $\alpha = 17°$

FIGURE 12.—Effect of area suction on the pressure distributions of the 35° swept-wing model; $\delta_F = 38°$, $U = 112$ feet per second.

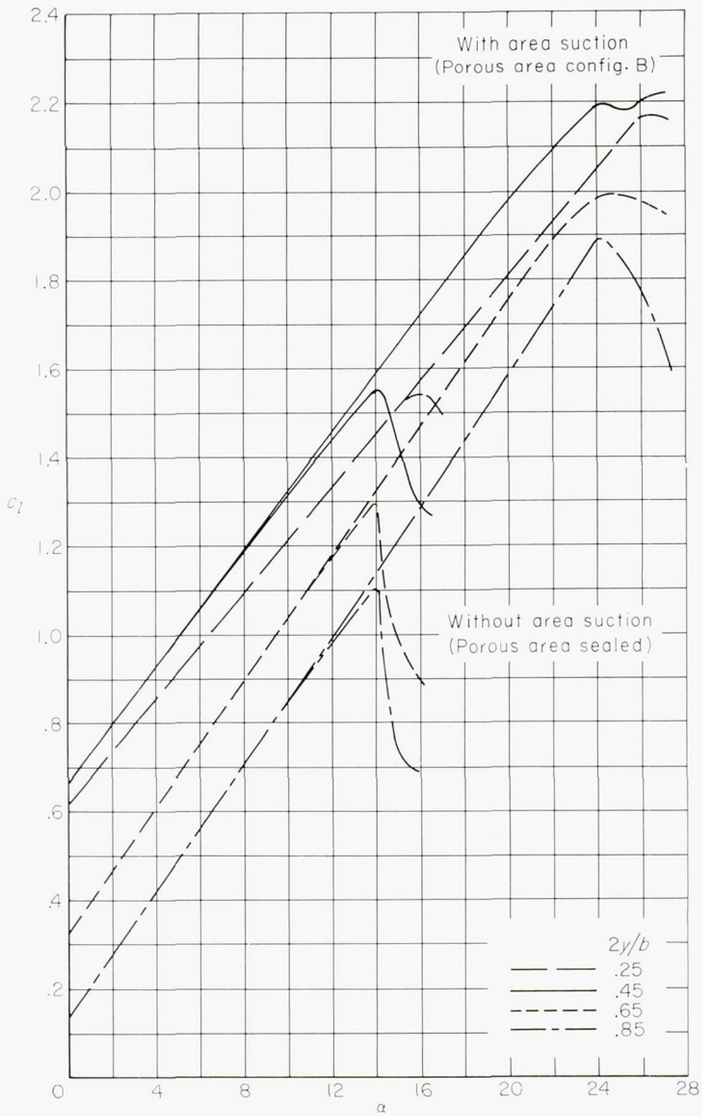


FIGURE 13.—Variation of section lift coefficients with angle of attack, with and without area suction: $\delta_F=38°$, $U=112$ feet per second.

primarily by the chordwise extent of porous area. Further, it should be pointed out that only a small increase in the maximum lift coefficient was obtained when configuration A was used in place of configuration B, even though the chordwise extent of porous area and the suction flow coefficients were approximately doubled. Based on these results, as well as on the pressure distributions, it is believed that air-flow separation from the trailing edge of the wing limited the maximum lift coefficient obtained with configuration A, and that further large increases in the maximum lift coefficient would not be expected by the use of area suction only at the leading edge.

The data presented in figure 14 show the variation of flow coefficient and duct pressure coefficient with lift coefficient for the different porous-area configurations tested at a free-stream velocity of 112 feet per second. Since the effects of free-stream velocity on the suction requirements were not known, additional data were obtained at higher free-stream velocities with porous-area configuration B and with the flaps deflected 38°. These data were obtained at free-stream velocities corresponding to those obtained at constant wing loadings in order to simulate the suction requirements of an airplane during a landing or take-off maneuver. These data are presented in figure 15 and in table V. Figure 15 shows the variation of suction flow coefficient and duct pressure coefficient with lift coefficient, and table V summarizes the measured power inputs and division of losses for several lift coefficients. It should be noted that the suction requirements presented in figures 14 and 15 are probably not the minimum values required at all of the lift coefficients. There are several reasons for this statement. First, a range of flow coefficients was run only at angles of attack near the maximum lift coefficient, thus the flow coefficients presented at lower lift coefficients are probably greater than those required to prevent air-flow separation. Second, the spanwise control of the duct pressures was very limited, and the duct pressure for the inboard sections of the wing could not be adequately reduced to compensate for the variation in peak surface pressures resulting from the span load distribution. Third, theoretically, a particular distribution of porosity exists for each lift coefficient and free-stream velocity to obtain a minimum flow coefficient; whereas in these tests only one design was used for all lift coefficients and free-stream velocities.

The data presented in figure 14 show that the flow requirements increased with increasing lift coefficients, and that for each porous area configuration, a particular value of lift coefficient was reached which could not be increased by increased suction; this lift coefficient was the maximum lift coefficient shown in figure 11. These data also show that for a given lift coefficient, the suction flow coefficient increased with increasing porous area extent, and the dashed curve in figure 14 (a) represents the probable variation of the minimum flow coefficient required to reach any given lift coefficient with the design of porous material tested. Further, it can be seen that for a given lift coefficient, the duct pressure coefficient remained essentially unchanged when the extent of porous area was increased, even though the required flow coefficient was increased. This resulted because the pressure drop through the porous material for all of the required suction-air velocities was relatively small at the chordwise location of the maximum surface pressure coefficient. Thus the duct pressure coefficient was essentially equal to the maximum surface pressure coefficient which was primarily a function of the angle of attack.

The data of figure 15 indicate that increasing the free-stream velocity did not affect the flow coefficient or duct pressure coefficient at a particular lift coefficient. Therefore, the suction power required should vary as the cube of the free-stream velocity; this is verified by the data given in table V.

**Comparison of experimental results with those computed by Thwaites' method.**—In figure 16 the experimentally minimized chordwise extents are compared with those predicted to be necessary for the same maximum lift coefficients. A comparison of the experimental and predicted chordwise extents of porous areas show that the chordwise extents for the maximum lift coefficients of 1.71, 1.87, and 2.03 were reasonably well predicted for the outboard portions

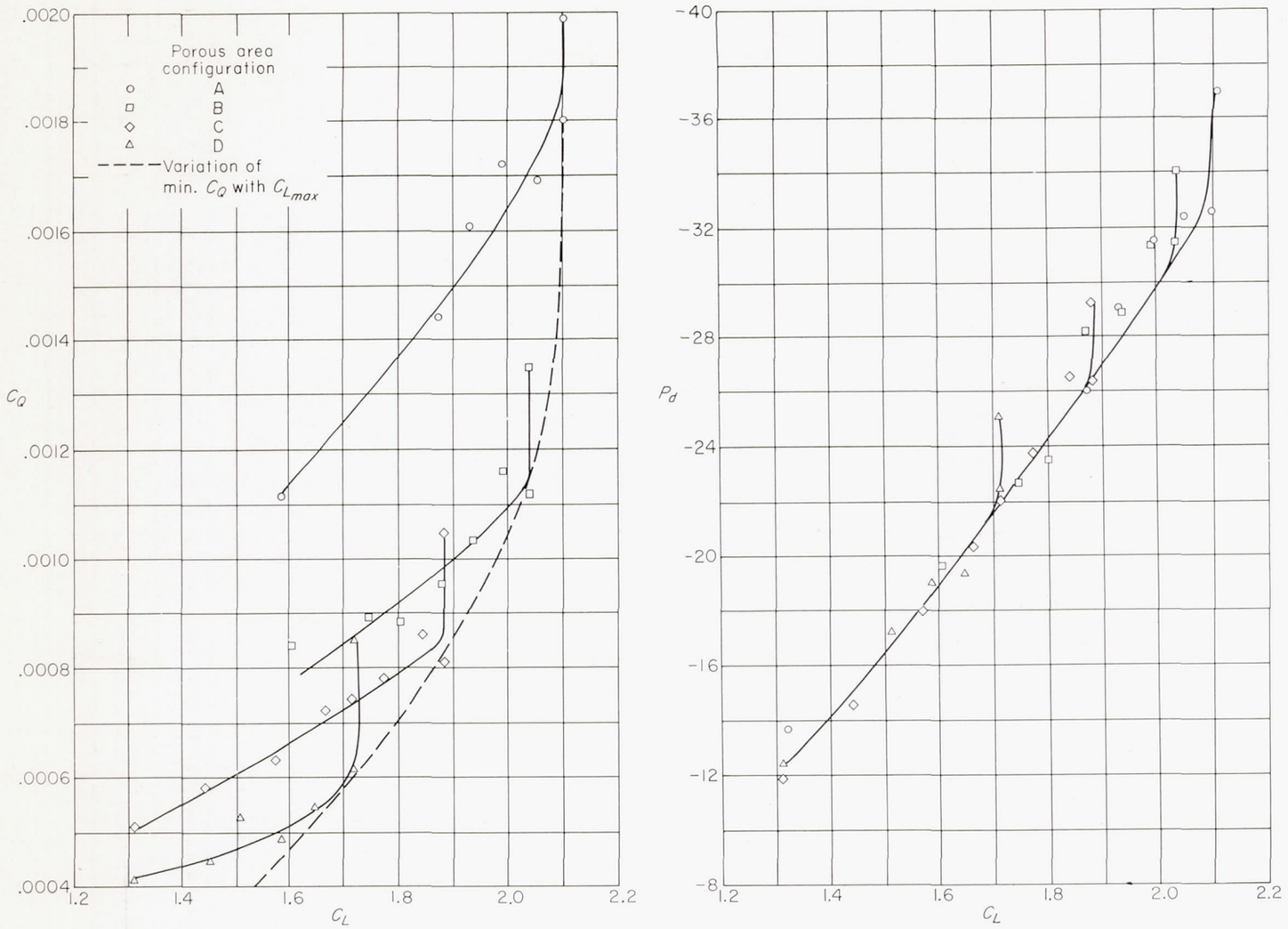


FIGURE 14.—Variation of suction requirements with lift coefficient for several porous area configurations on 35° swept-wing model; $U=112$ feet per second; $\delta_F=38°$.

of the wing where the initial separation occurred. The chordwise extents of porous area required for the inboard portions of the wing were considerably less than those predicted to be necessary. This difference is believed to be attributable to the spanwise flow of the boundary layer and its effect on the maximum lift characteristics of the airfoil sections on a sweptback wing; this effect is discussed in reference 6 for a 45° sweptback wing.

The chordwise extent required on the outboard portion of the wing for a maximum lift coefficient of 2.13 was about twice that predicted to be necessary. It was noted in a previous section that it was believed this maximum lift coefficient was limited by air-flow separation from the trailing edge of the wing rather than from the leading edge; hence, the chordwise extent required was greater than that predicted to be necessary based on considerations of leading-edge separation alone.

The variation of the experimental flow coefficient with lift coefficient is compared in figure 17 with the values computed to be necessary. The experimental curve used in this figure is the envelope of the curves of figure 14 (a) for a free-stream velocity of 112 feet per second. Two curves are shown for the computed values; one curve is for the values computed from the predicted chordwise extents of porous area and the suction-air velocities calculated to be necessary by the equations set forth by Thwaites. The other curve is 12 times the flow coefficient computed to be necessary, and this curve represents the magnitude of the difference between the computed and experimental results. Figure 18 is presented to show the spanwise distribution of the average suction-air velocities at a lift coefficient of 1.93 and a free-stream velocity of 112 feet per second. These suction-air velocities were calculated from the measured external and duct pressures at each of the four spanwise measuring stations. Included in figure 18 for comparative purposes is the spanwise distribution of suction-air velocity used for the design of the porous material. It can be seen in this figure that on the outboard portion of the wing the average suction-air velocities were of the order of those expected to be necessary (based on previous tests with area suction), values about 12 times those computed from Thwaites' equations. However, on the inboard portion of the wing, the suction-air velocities were considerably higher than had been anticipated. It is believed that these higher values were caused by the inadequate control of the spanwise duct pressure that was available on the model. Thus, it can be surmised that it was fortuitous


FIGURE 15.—Effect of free-stream velocity on the variation of suction flow coefficient and duct pressure coefficient with lift coefficient for 35° swept-wing model; porous area configuration B, $\delta_F = 38°$.

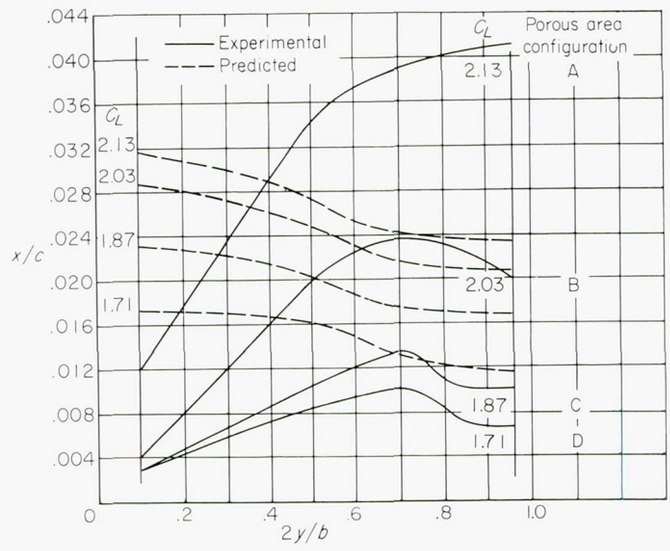


FIGURE 16.—Comparison of experimentally minimized chordwise extents of porous areas with those predicted to be necessary; $\delta_F = 38°$.

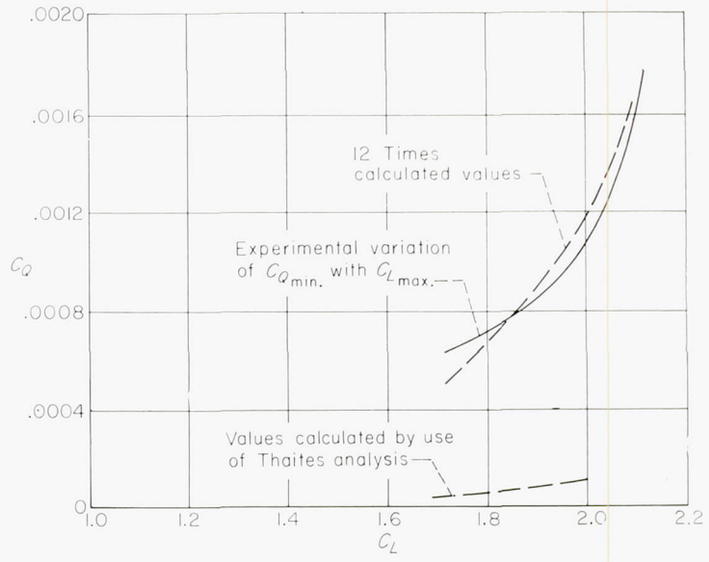


FIGURE 17.—Comparison of experimental and predicted flow coefficients for the model; $\delta_F = 38°$. $U = 112$ feet per second.

that the total flow coefficient was 12 times the computed value (fig. 17).

It is also of interest to compare the chordwise distribution of suction-air velocity with that used in the design of the porous leading edge. For this purpose, the 0.85 semispan station was chosen, and the chordwise distribution of suction-air velocity at three flow coefficients is shown in figure 19 for the design lift coefficient of 1.93 and free-stream velocity of 112 feet per second. These flow coefficients represent values above the minimum required, the minimum required, and a value below the minimum required. Also included in this figure are the lift coefficients measured at these three flow coefficients. It can be seen from this figure that a loss in lift was encountered when the flow coefficient was reduced to the point where the suction-air velocity near the leading edge was less than the value used in the design. It cannot be determined, however, whether the suction-air velocities aft of the leading edge could have been reduced by redesigning the porous material.

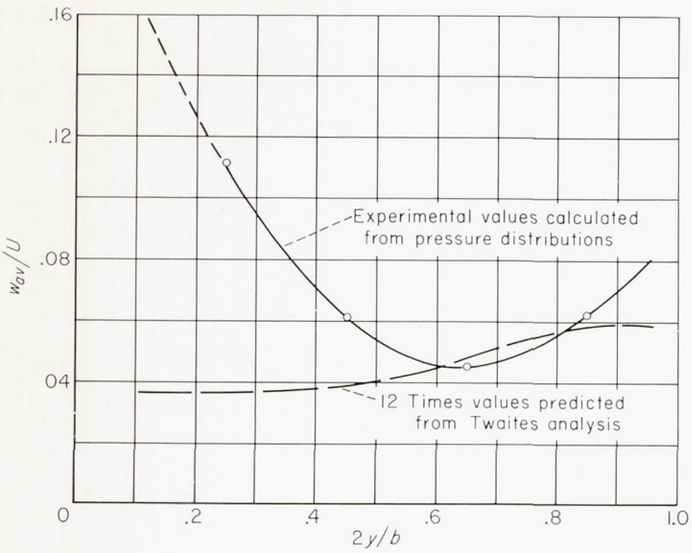


FIGURE 18.—Comparison of experimental and theoretical ratios of average suction-air velocity to free-stream velocity; $C_L = 1.93$; $U = 112$ feet per second.

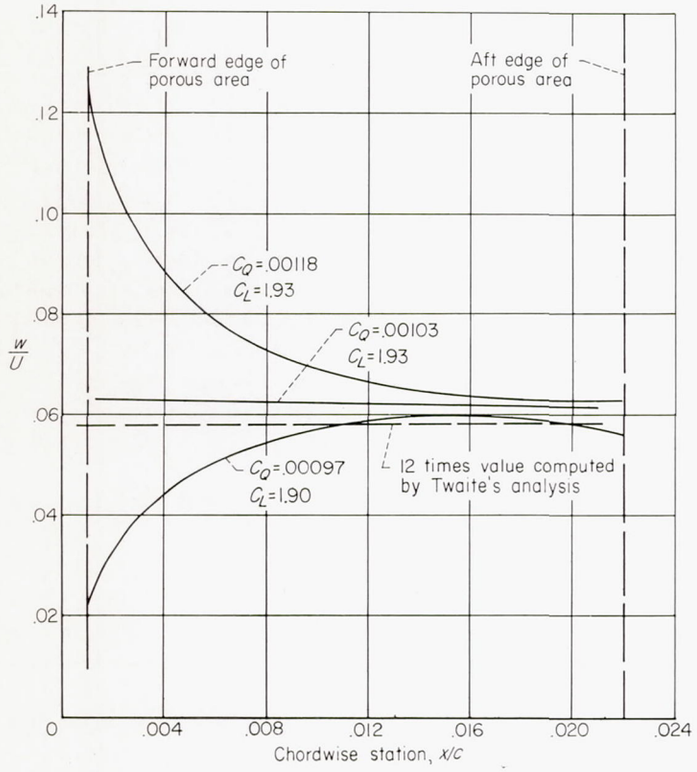


FIGURE 19.—Ratio of suction-air to free-stream velocity at 0.85 semi-span station, computed from surface pressure distributions; $\alpha = 22.2°$, $U = 112$ feet per second, porous area configuration B, flap deflected 38°.

### FLIGHT TESTS

**Lift characteristics of the airplane with a porous leading edge.**—The lift characteristics of the test airplane with the full-span porous leading edge are shown in figure 20 for conditions of maximum available suction flow, and for suction off with the porous surface open and the ducts closed. Also included in this figure for comparative purposes are the results of the wind-tunnel investigation for a similar

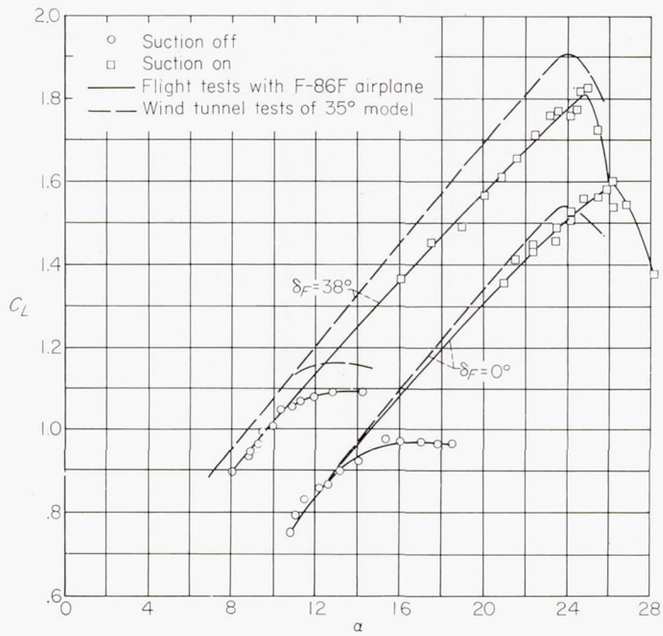


FIGURE 20.—Comparison of flight results with those obtained in the wind tunnel; porous area configuration B.

configuration (porous-area configuration B). It should be pointed out that the wind-tunnel data have been corrected to trimmed conditions for a center-of-gravity position similar to that of the flight tests. For the flaps-retracted condition, good agreement is obtained between the flight and wind-tunnel results, with the flight installation providing a slightly higher value of maximum lift coefficient. For the flaps-down condition, the agreement is less satisfactory, with the flight data showing lower lift throughout the angle-of-attack range. This difference might be explained partially by differences in the configurations of the wind-tunnel model and the F–86 airplane. The wind-tunnel model had no landing gear, but in its place were the model support struts; in addition, the landing-gear wells were closed. The fuselage of the wind-tunnel model bore no resemblance to that of the F–86 airplane; it had a circular cross section with a smaller width and a higher fineness ratio, and the wing of the model was mounted on the fuselage center line instead of the low position. Flight tests with the landing gear of the airplane extended and retracted indicated that the major portion of the difference in lift at the lower angles of attack is the result of a loss of flap effectiveness due to the extended gear and open gear wells.

The stall with suction, despite the extremely nose-high attitude due to angle of attack and the relatively high engine power required, was not considered objectionable by the pilot, but a lack of stall warning was noted. Although the stall was abrupt, the accompanying roll-off and pitch-up were of a controllable magnitude. With flaps and gear retracted, the stall was considered extremely mild and was characterized by a slight pitch-up and no roll-off. Just prior to the stall with maximum suction power, tufts on the wing surface indicated a strong spanwise flow in the boundary layer over the ailerons. With an increase in angle of attack, the flow at the outboard portions of the trailing edge appeared to separate, the area of separation rapidly spreading

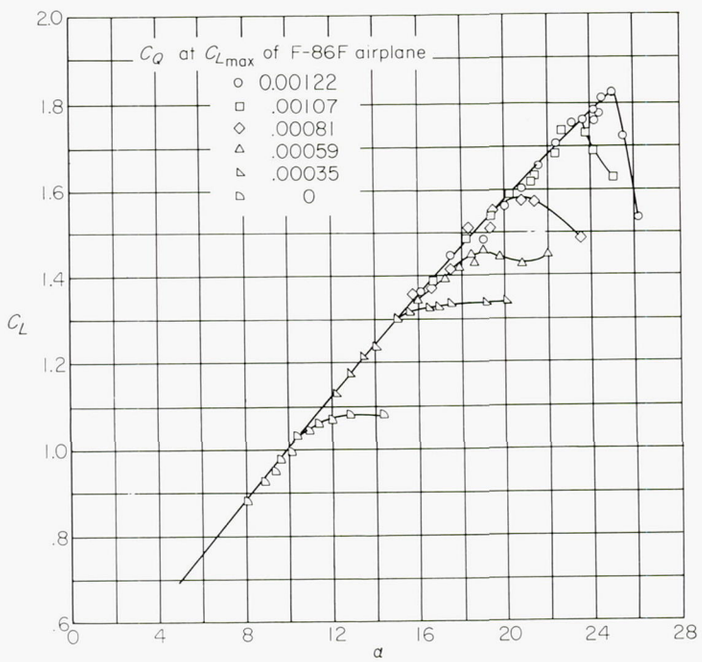


FIGURE 21.—Variation of lift coefficient with angle of attack for several values of suction flow coefficient; $\delta_F = 38°$, porous area configuration B.

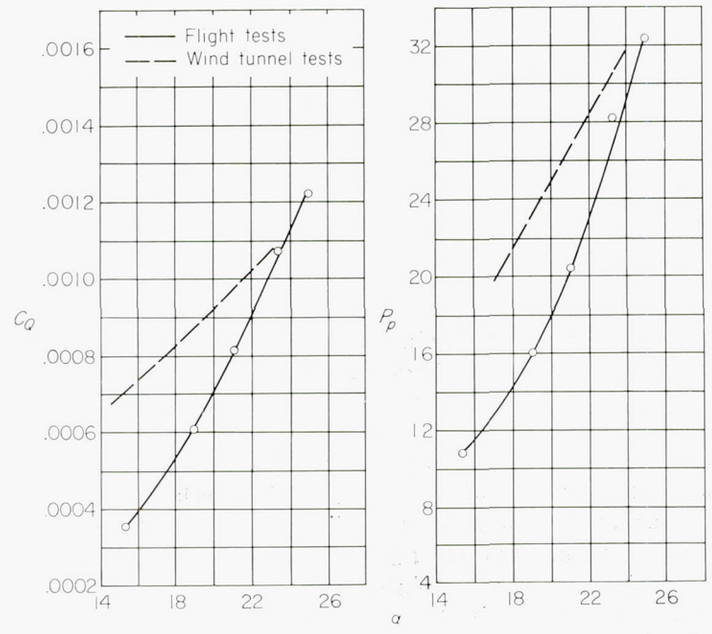


FIGURE 22.—Comparison of suction pumping requirements in the flight tests and wind-tunnel tests; $\delta_F = 38°$, porous area configuration B.

forward and inboard as the stall was approached. However, it appeared that while a trailing-edge type of stall was imminent, the final complete flow separation was triggered by a disturbance occurring at the leading edge at about the 70-percent semispan station. Based on these observations, as well as on the wind-tunnel results with a larger open chordwise extent of porous area, it seems doubtful that further increases in suction flow or refinements of the porous-area configuration would produce large increases in maximum lift coefficient. In contrast to the stall with area suction, the pilot was not able to define the stall point of the airplane

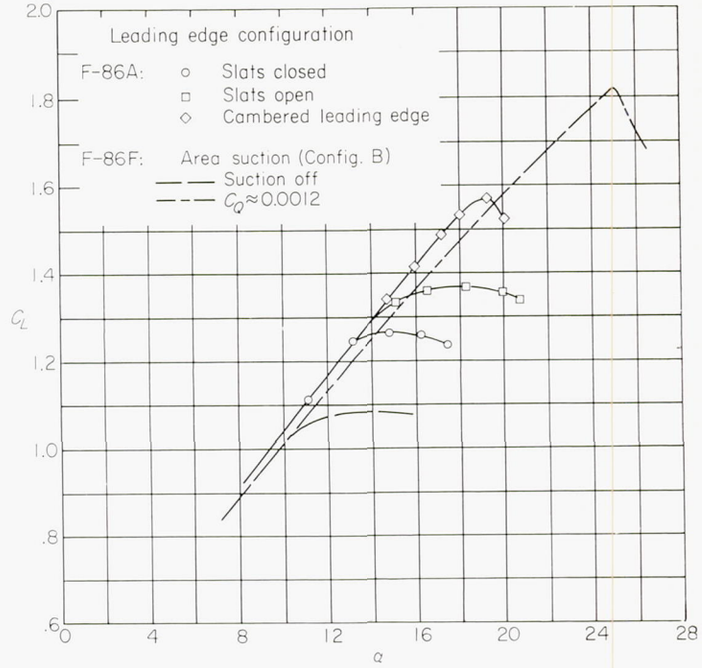


FIGURE 23.—Comparison of lift coefficients obtained with various leading-edge high-lift devices; $\delta_F = 38°$.

with suction off. Buffeting and lateral unsteadiness appeared at a speed corresponding to an angle of attack of 11° and increased gradually with increasing angle of attack. Due to the lack of reference with which to gage rate of sink, it was not obvious to the pilot that the airplane was beyond the maximum lift coefficient at angles of attack above 13°. With suction off, tufts indicated that flow separation appeared first from the leading edge at mid-semispan and spread slowly outboard and inboard.

The effects of varying flow coefficient upon the lift characteristics of the airplane with flaps deflected are shown in figure 21. With a reduction in flow coefficient, the stalling behavior of the airplane gradually changed from the abrupt stall exhibited at maximum flow to the mild type of stall that occurred with suction off.

**Suction requirements of porous leading edge.**—The variations of flow coefficient and pump inlet pressure coefficient with angle of attack are shown in figure 22 for porous-area configuration B with the trailing-edge flaps deflected. To obtain a further comparison of the flight-test and wind-tunnel-test results, figure 22 also includes the suction requirements, measured in the wind tunnel for porous-area configuration B with flaps deflected, at a wing loading of 40 pounds per square foot. These suction requirements are compared on the basis of angle of attack rather than lift coefficient because of the previously noted differences in lift coefficient. Comparison of the flight and wind-tunnel suction requirements indicates a close agreement near the maximum effectiveness of the leading-edge suction installation; however, for angles of attack below 24°, the flight installation appeared to require considerably less flow than was required in the wind tunnel. The exact reason for this discrepancy is not known; however, in the flight tests there was a better spanwise control of the duct pressure distribution. In addition, as was noted previously, the minimum

suction requirements were not completely evaluated in the wind tunnel at angles of attack below those for maximum lift coefficient.

**Comparison of lift characteristics of various leading-edge-type high-lift devices.**—The lift characteristics of the F–86A airplane having the trailing-edge flap deflected with a slatted leading edge extended and retracted and with a leading edge modified to include increased camber and leading-edge radius are compared in figure 23 with those of the F–86F airplane having the porous leading edge. Although slight differences were obtained in the lifts measured at angles of attack below the respective maximum lift coefficients, it is felt that a comparison of the maximum lift coefficients is indicative of the relative lift capabilities of the various leading-edge devices. These maximum lift coefficients, $C_{L_{max}}$, are compared in the following table along with the pilot's opinions of the stalling characteristics of each device:

| Configuration | $C_{L_{max}}$ | Stalling characteristics |
|---|---|---|
| Porous leading edge, suction on. | 1. 82 | Controllable, but no stall warning. |
| Cambered leading edge | 1. 58 | Not controllable and no stall warning. |
| Normal leading edge, slats extended. | 1. 36 | Controllable and adequate stall warning. |
| Normal leading edge, slats closed. | 1. 27 | Controllable and adequate stall warning. |
| Porous leading edge, suction off. | 1. 08 | Controllable and adequate stall warning. |

It is evident that the area-suction leading edge is a considerably more effective means of increasing the maximum lift of a wing than the other high-lift devices. It can also be seen that there was a reduction in the maximum lift coefficient when the normal leading edge (slats closed) was replaced by the porous leading edge and no suction was applied. A similar loss was measured in the wind-tunnel tests and was attributed to circulation of air through the porous material.

**Landing and take-off performance.**—The effects of the porous leading-edge installation upon the landing and take-off characteristics of the F–86F airplane are reported here only in terms of a pilot's preliminary evaluation; no precise measurements of speeds or distances were taken. The performances quoted refer to the F–86A and F–86F airplanes without external stores at normal take-off and landing weights. This evaluation is subject to the following factors which apply to the F–86 airplane as a type: (1) The airplane is limited to a maximum ground angle of attack of about 15° and has no protective tail bumper, and (2) at the highest angles of attack which were attainable in the landing approach with the suction equipment, visibility was objectionably limited.

The take-off characteristics of the F–86F airplane with the porous leading-edge installation were considered very similar to those of the normal F–86A or F–86F with slatted leading edge. At normal gross weight for take-off, the nose wheel lifted off at about 90 knots, indicated airspeed, and the airplane became airborne at about 105 knots. After take-off, however, an extremely nose-high attitude could be attained which resulted in a steep angle of climb. At a climb speed of 110 knots, flaps and gear up, under no-wind conditions, an altitude of 1,000 feet could be easily attained before reaching the end of an 8,000-foot runway.

The main advantage of the high maximum lift due to suction in the landing approach was the increased ability to maneuver; however, the high engine speed required to maintain adequate suction (about 70 percent of the maximum) made it difficult to lose altitude and still approach at a low airspeed. The best approach speed for a normal descending type of approach seemed to be 112 knots. For a power-on, carrier-type approach, a favorable speed was 105 knots. Comparable speeds for the F–86A or F–86F airplane with slats are about 120 and 115 knots, respectively. The touchdown speed with suction applied was about 104 knots and was limited by poor visibility and a fear of dragging the tail pipe. It is obvious that the reduction in stalling speed afforded by this leading-edge-suction installation cannot be fully utilized on this airplane to decrease the landing speed.

**High-speed performance.**—Several flights were made at altitudes up to 35,000 feet and speeds up to those corresponding to a Mach number of 0.9 in order to check the effects of the suction equipment and porous leading edge under these conditions. Determination of the effects of the porous leading edge on the high-speed drag of the airplane was made difficult by the fact that the contribution of drag from the pump pod was unknown and apparently varied with operation of the suction equipment. Therefore, drag measurements were obtained with the porous leading edge, suction on and suction off, and with a production leading edge installed, and the pump operative and inoperative. The results of these tests indicated that flow through the porous leading edge had little effect on the high-speed flight drag of the test airplane.

A check of the buffeting characteristics of the airplane in turns at 35,000 feet revealed no measurable change in the buffet boundary due to the porous leading edge, suction on or off, from that of an F–86 airplane with a slatted leading edge. At Mach numbers from 0.60 to 0.80 and at lift coefficients above the buffet boundary, there was some evidence of an increase in buffet amplitude with the suction equipment operating at maximum power. A low-frequency buffeting (7 to 8 cycles per second) accompanied an apparent stalling of the pump and surging of the static pressure in the duct which resulted in intermittent flow separation on the wing. A similar condition could be found in turns at low altitudes at indicated airspeeds of 200 to 300 knots. This phenomenon has not been fully explained; however, it is not considered particularly significant since the conditions are well beyond the design operating range of the pumping equipment.

**Serviceability of the porous leading edge.**—During the early tests with the porous leading edge, disappointingly low values of maximum lift coefficient were obtained. An examination of the behavior of tufts on the wing showed that the stall was being precipitated by a premature localized flow separation which appeared immediately behind the juncture of the two outer porous panels on the right wing. Yawing the airplane to the right duplicated this condition on the left wing. Removal of portions of the nose ribs at the junctures of the leading-edge panels, effectively eliminating discontinuities in the porous area which were about ¾ of an inch in width, resulted in an increase in maximum lift

coefficient from 1.45 to 1.82. In contrast to the sensitivity of the installation to small areas of reduced porosity was its apparent insensitivity to wing surface condition near the leading edge. In the original condition, numerous large defects in contour existed in the modified portion of the leading edge. During the course of the tests, a major portion of the defects was removed by refairing the surface immediately aft of the porous area; however, no changes in the aerodynamic characteristics of the wing were noted.

One flight was devoted to a determination of the effects of rain on the operation of the suction equipment and upon the lift of the wing. A series of stalls made in moderate to heavy rain revealed no significant effects on either the lift coefficient for the stall or the power required. Unfortunately, these flights were made early in the program, before the highest lifts were being obtained, so any small effects of rain might have been masked.

After approximately six months of operation of the aircraft (60 hours of flight), flow-quantity and pressure measurements revealed no evidence of decreasing porosity of the leading-edge material. Other than covering the leading edges when the airplane was inactive, little special attention was given to their maintenance.

## CONCLUDING REMARKS

The results of the wind-tunnel and flight tests of a 35° sweptback wing airplane having area suction applied to the leading edge of the wing showed that the use of area suction increased the maximum lift coefficient more than 50 percent. Although the maximum lift coefficients were obtained with relatively low flow coefficients, relatively high pumping pressure ratios were required. Good agreement was obtained in the comparison of the wind-tunnel results with those measured in flight. The increase in the maximum lift coefficient obtained with area suction applied to the leading edge of the wing of the airplane was greater than that obtained by the use of a slatted leading edge or a leading edge having camber and increased leading-edge radius. Further, there appeared to be no detrimental effects of the area-suction installation on the operation or performance of the airplane.

AMES AERONAUTICAL LABORATORY
NATIONAL ADVISORY COMMITTEE FOR AERONAUTICS
MOFFETT FIELD, CALIF., *March 2, 1956*

## REFERENCES

1. Thwaites, B.: A Theoretical Discussion of High-Lift Aerofoils With Leading-Edge Porous Suction. R. & M. No. 2242, British A. R. C., July, 1946.
2. Nuber, Robert J., and Needham, James R., Jr.: Exploratory Wind-Tunnel Investigation of the Effectiveness of Area Suction in Eliminating Leading-Edge Separation over an NACA $64_1$A212 Airfoil. NACA TN 1741, 1948.
3. Pankhurst, R. C., Raymer, W. G., and Devereux, A. N.: Wind-Tunnel Tests of the Stalling Properties of an 8-Percent Thick Symmetrical Section With Continuous (Distributed) Nose Suction. R. & M. No. 2666, British A. R. C., 1953.
4. Dannenberg, Robert E., and Weiberg, James A.: Section Characteristics of a 10.5-Percent-Thick Airfoil With Area Suction as Affected by Chordwise Distribution of Permeability. NACA TN 2847, 1952.
5. Weiberg, James A., and Dannenberg, Robert E.: Section Characteristics of an NACA 0006 Airfoil With Area Suction Near the Leading Edge. NACA TN 3285, 1954.
6. Hunton, Lynn W.: Effects of Finite Span on the Section Characteristics of Two 45° Sweptback Wings of Aspect Ratio 6. NACA TN 3008, 1953.
7. Campbell, G. W., Peskin, B. A., and Przybylowicz, J. A.: Boundary Layer Control by Porous Area Suction on the Wing Leading Edges of an F–86F Airplane. WADC TR 54–290, Wright Air Development Center, June 1954

TABLE I.—DIMENSIONS OF THE TEST VEHICLES

| | |
|---|---|
| Wing | |
| Total area, sq ft | 287.9 |
| Span, ft | 37.1 |
| Aspect ratio | 4.79 |
| Taper ratio | 0.51 |
| Mean aerodynamic chord (wing station 98.7 in.), $\bar{c}$ ft | 8.1 |
| Dihedral angle, deg | 3.0 |
| Sweepback of leading edge, deg | 37.7 |
| Sweepback of 0.25-chord line, deg | 35.0 |
| Aerodynamic and geometric twist, deg | 2.0 |
| Root airfoil section (normal to 0.25-chord line) | NACA 0012–64 (modified) |
| Tip airfoil section (normal to 0.25-chord line) | NACA 0011–64 (modified) |
| Horizontal tail | |
| Total area, sq ft | 35.0 |
| Span, ft | 12.7 |
| Aspect ratio | 4.65 |
| Taper ratio | 0.45 |
| Dihedral angle, deg | 10.0 |
| Mean aerodynamic chord (horizontal-tail station 33.54 in.) ft | 2.9 |
| Sweepback of 0.25-chord line, deg | 34.6 |
| Airfoil section (parallel to center line) | NACA 0010–64 |
| Vertical tail of the F–86 airplanes | |
| Total area, sq ft | 34.4 |
| Span, ft | 7.5 |
| Aspect ratio | 1.74 |
| Taper ratio | 0.36 |
| Sweepback of 0.25-chord line, deg | 35.0 |
| Distance between wing $\frac{\bar{c}}{4}$ and horizontal tail $\frac{\bar{c}}{4}$, ft | 18.1 |

TABLE II.—COORDINATES OF THE WING AIRFOIL SECTIONS NORMAL TO THE WING QUARTER-CHORD LINE AT TWO SPAN STATIONS

(a) Coordinates for normal F–86 wing

| Section at 0.467 semispan | | | Section at 0.857 semispan | | |
|---|---|---|---|---|---|
| Chordwise station in. | z, in. | | Chordwise station in. | z, in. | |
| | Upper surface | Lower surface | | Upper surface | Lower surface |
| 0 | 0.231 | ------ | 0 | −.098 | ------ |
| .119 | .738 | −0.307 | .089 | .278 | −0.464 |
| .239 | .943 | −.516 | .177 | .420 | −.605 |
| .398 | 1.127 | −.698 | .295 | .562 | −.739 |
| .597 | 1.320 | −.895 | .443 | .701 | −.879 |
| .996 | 1.607 | −1.196 | .738 | .908 | −1.089 |
| 1.992 | 2.104 | −1.703 | 1.476 | 1.273 | −1.437 |
| 3.984 | 2.715 | −2.358 | 2.952 | 1.730 | −1.878 |
| 5.976 | 3.121 | −2.811 | 4.428 | 2.046 | −2.176 |
| 7.968 | 3.428 | −3.161 | 5.903 | 2.290 | −2.401 |
| 11.952 | 3.863 | −3.687 | 8.855 | 2.648 | −2.722 |
| 15.936 | 4.157 | −4.064 | 11.806 | 2.911 | −2.944 |
| 19.920 | 4.357 | −4.364 | 14.758 | 3.104 | −3.102 |
| 23.904 | 4.480 | −4.573 | 17.710 | 3.244 | −3.200 |
| 27.888 | 4.533 | −4.719 | 20.661 | 3.333 | −3.250 |
| 31.872 | 4.525 | −4.800 | 23.613 | 3.380 | −3.256 |
| 35.856 | 4.444 | −4.812 | 26.564 | 3.373 | −3.213 |
| 39.840 | 4.299 | −4.758 | 29.516 | 3.322 | −3.126 |
| 43.825 | 4.081 | −4.638 | 32.467 | 3.219 | −2.989 |
| 47.809 | 3.808 | −4.452 | 35.419 | 3.074 | −2.803 |
| 51.793 | 3.470 | −4.202 | 38.370 | 2.885 | −2.574 |
| 55.777 | 3.066 | −3.891 | 41.322 | 2.650 | −2.302 |
| 59.761 | 2.603 | −3.521 | 44.273 | 2.374 | −1.986 |
| [a] 63.745 | 2.079 | −3.089 | [a] 47.225 | 2.054 | −1.625 |
| 83.681 | −.740 | ------ | 63.031 | .321 | ------ |
| Leading edge radius: 1.202; center at 1.201, 0.216 | | | Leading edge radius: 0.822; center at 0.822, −0.093 | | |

[a] Straight lines to trailing edge.

## TABLE II.—COORDINATES OF THE WING AIRFOIL SECTIONS NORMAL TO THE WING QUARTER-CHORD LINE AT TWO SPAN STATIONS

(b) Coordinates for the cambered leading edge of the F–86A airplane

| Section at 0.467 semispan | | | Section at 0.857 semispan | | |
|---|---|---|---|---|---|
| Chordwise station in. | $z$, in. | | Chordwise station in. | $z$, in. | |
| | Upper surface | Lower surface | | Upper surface | Lower surface |
| −1.692 | −1.445 | ------ | −1.250 | −1.359 | ------ |
| −1.273 | −.348 | −2.552 | −.934 | −.495 | −2.192 |
| −.855 | .222 | −2.898 | −.619 | −.099 | −2.454 |
| −.436 | .629 | −3.114 | −.304 | .197 | −2.609 |
| −.018 | .969 | −3.272 | .011 | .456 | −2.701 |
| .400 | 1.266 | −3.391 | .326 | .675 | −2.769 |
| .819 | 1.527 | −3.473 | .641 | .867 | −2.796 |
| 1.237 | 1.760 | −3.523 | .956 | 1.040 | −2.813 |
| 1.655 | 1.952 | −3.549 | 1.272 | 1.189 | −2.821 |
| 1.992 | 2.104 | ------ | 1.476 | 1.273 | ------ |
| 2.074 | ------ | −3.552 | 1.587 | ------ | −2.813 |
| 2.911 | ------ | −3.531 | 2.217 | ------ | −2.787 |
| 4.166 | ------ | −3.481 | 3.163 | ------ | −2.742 |
| 6.258 | ------ | −3.472 | 4.739 | ------ | −2.709 |
| 8.350 | ------ | −3.542 | 6.314 | ------ | −2.712 |
| 10.442 | ------ | −3.657 | 7.890 | ------ | −2.751 |
| 14.626 | ------ | −3.956 | 9.466 | ------ | −2.808 |
| 15.936 | ------ | −4.064 | 11.042 | ------ | −2.885 |
| | | | 11.806 | ------ | −2.944 |
| Leading edge radius: 1.674; center at −0.018, −1.445 | | | Leading edge radius: 1.261; center at 0.011, −1.359 | | |

## TABLE III.—LOCATION OF SURFACE PRESSURE ORIFICES ON WIND-TUNNEL MODEL

[Position of orifices, fraction of streamwise chord]

| $0.25\frac{b}{2}$ station | | $0.45\frac{b}{2}$ station | | $0.65\frac{b}{2}$ and $0.85\frac{b}{2}$ station | |
|---|---|---|---|---|---|
| Upper surface | Lower surface | Upper surface | Lower surface | Upper surface | Lower surface |
| 0 | ------ | 0 | ------ | 0 | ------ |
| .0025 | 0.0025 | .0025 | 0.0025 | .0025 | 0.0025 |
| .005 | .005 | .005 | .005 | .005 | .005 |
| .01 | .01 | .01 | .01 | .01 | .01 |
| .015 | .015 | .015 | .015 | .015 | .015 |
| .02 | .02 | .02 | .02 | .02 | .02 |
| .025 | .025 | .025 | .025 | .025 | .025 |
| .035 | .035 | .035 | .035 | .035 | .035 |
| .05 | .05 | .05 | .05 | .05 | .05 |
| .075 | .075 | .075 | .075 | .075 | .075 |
| .1 | .1 | .1 | .1 | .1 | .1 |
| .15 | .15 | .15 | .15 | .15 | .15 |
| .2 | .2 | .2 | .2 | .2 | .2 |
| .3 | .3 | .3 | .3 | .3 | .3 |
| .4 | .4 | .4 | .4 | .4 | .4 |
| .5 | .5 | .5 | .5 | .5 | .5 |
| .6 | .6 | .6 | .6 | .6 | .6 |
| .7 | .7 | .7 | .7 | .7 | .7 |
| .765 | .8 | .74 | .82 | .8 | .8 |
| .78 | .915 | .755 | .98 | .9 | .9 |
| .81 | .98 | .788 | | .975 | .975 |
| .92 | | .85 | | | |
| .98 | | .98 | | | |

## TABLE IV.—CONFIGURATIONS OF THE WIND-TUNNEL MODEL TESTED AND THE TEST CONDITIONS

| Porous-leading-edge configuration | $\delta_f$, deg | Suction or no suction | $U$, ft/sec | $W/S$ lb/sq ft |
|---|---|---|---|---|
| Sealed | 0 | ------ | 112 | varied |
| Sealed | 38 | ------ | 112 | varied |
| B, root valves closed | 38 | none | 112 | varied |
| A | 38 | suction | 112 | varied |
| B | 38 | suction | 112 | varied |
| B | 38 | suction | 112 to 162 | 30 |
| B | 38 | suction | 129 to 180 | 40 |
| B | 38 | suction | 145 to 180 | 50 |
| C | 38 | suction | 112 | varied |
| D | 38 | suction | 112 | varied |
| A | 0 | suction | 112 | varied |
| B | 0 | suction | 112 | varied |

## TABLE V.—POWER REQUIREMENTS FOR 35° SWEPT-WING MODEL WITH POROUS-AREA CONFIGURATION B AND FLAPS DEFLECTED 38°

| $C_L$ | $U$, ft/sec | $C_Q$ | Measured power input, hp | Suction power, hp | Pump loss, hp | Duct loss, hp |
|---|---|---|---|---|---|---|
| Wing loading, 30 lb/sq ft | | | | | | |
| 1.99 | 112 | 0.00109 | 56 | 36 | 17 | 3 |
| 1.85 | 116 | .00096 | 44 | 30 | 12 | 2 |
| 1.72 | 121 | .00090 | 35 | 23 | 10 | 2 |
| 1.59 | 126 | .00080 | 30 | 20 | 8 | 2 |
| Wing loading, 40 lb/sq ft | | | | | | |
| 1.99 | 129 | .00108 | 81 | 47 | 27 | 7 |
| 1.85 | 134 | .00095 | 70 | 41 | 23 | 6 |
| 1.72 | 140 | .00087 | 57 | 35 | 17 | 5 |
| 1.60 | 145 | .00079 | 49 | 30 | 14 | 5 |
| Wing loading, 50 lb/sq ft | | | | | | |
| 1.99 | 145 | .00111 | 160 | 80 | 63 | 17 |

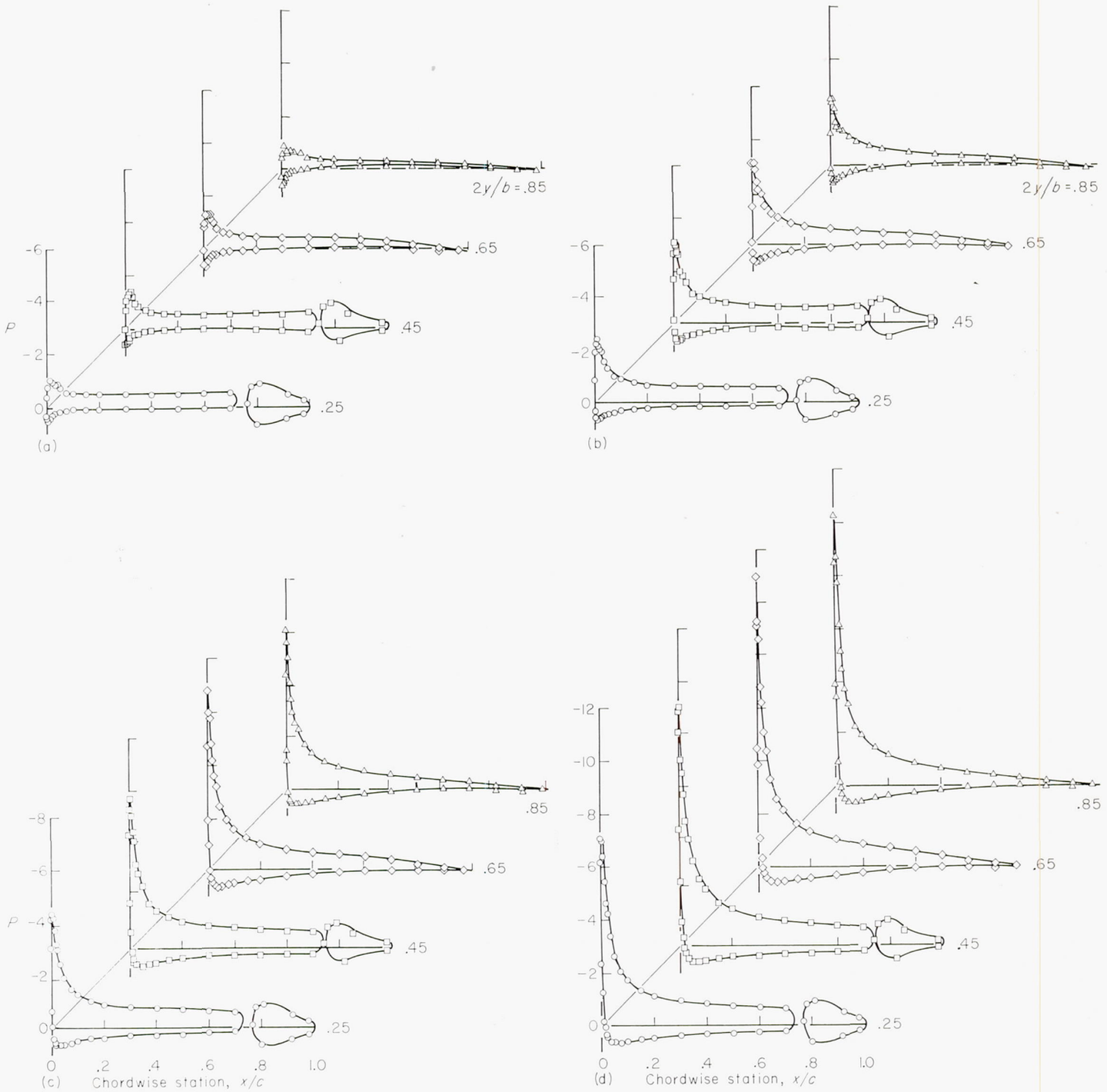


(a) $\alpha = 0.3°$
(b) $\alpha = 4.5°$
(c) $\alpha = 8.7°$
(d) $\alpha = 12.8°$

FIGURE 24.—Chordwise pressure distributions of the 35° swept-wing model with porous leading edge sealed; $\delta_F = 38°$, $U = 112$ feet per second.

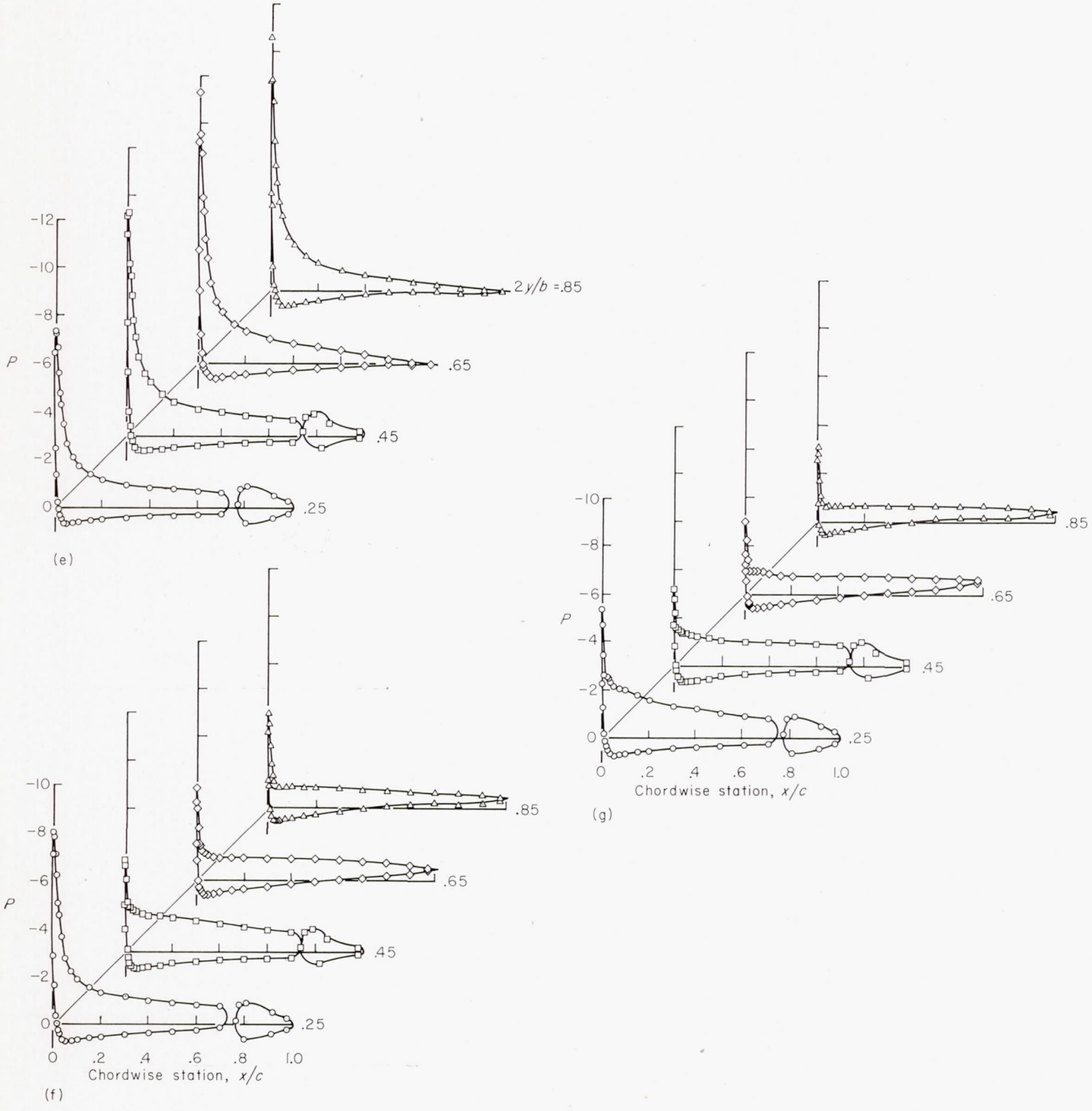


(e) $\alpha = 13.9°$
(f) $\alpha = 14.8°$
(g) $\alpha = 16.7°$

FIGURE 24.—Concluded.

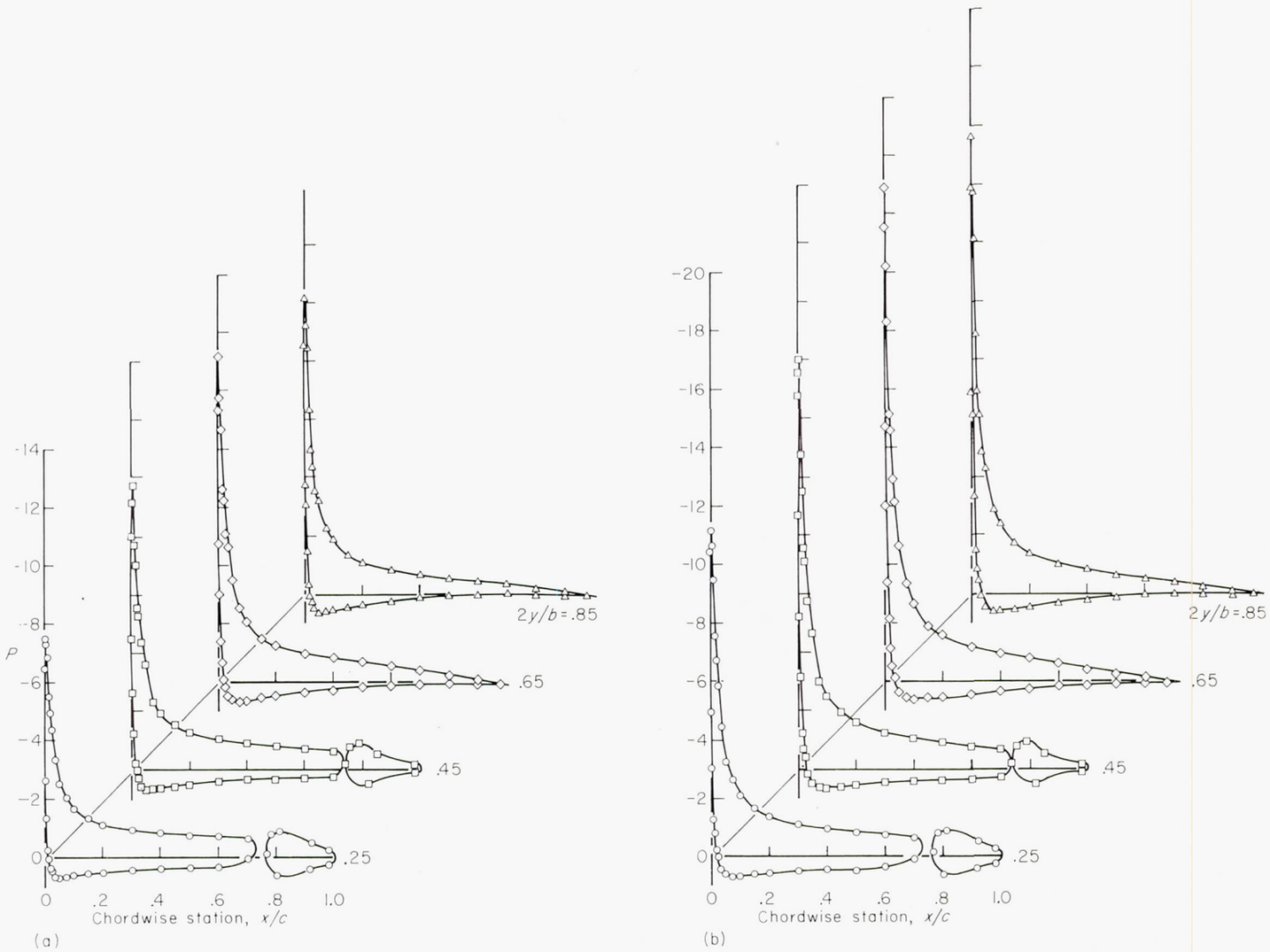


(a) $\alpha = 12.9°$ (b) $\alpha = 17.0°$

FIGURE 25.—Chordwise pressure distributions of the 35° swept-wing model with area suction applied and $\delta_F = 38°$; porous area configuration B, $U = 112$ feet per second.

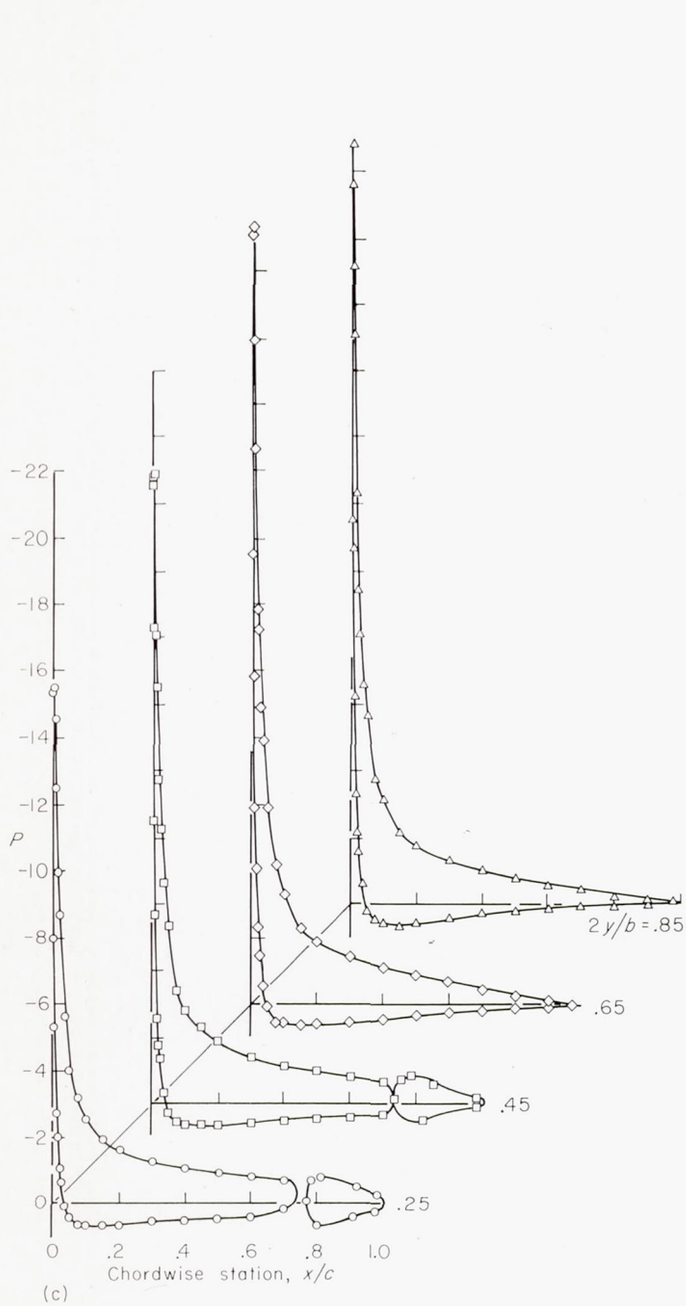


(c) $\alpha = 22.2°$

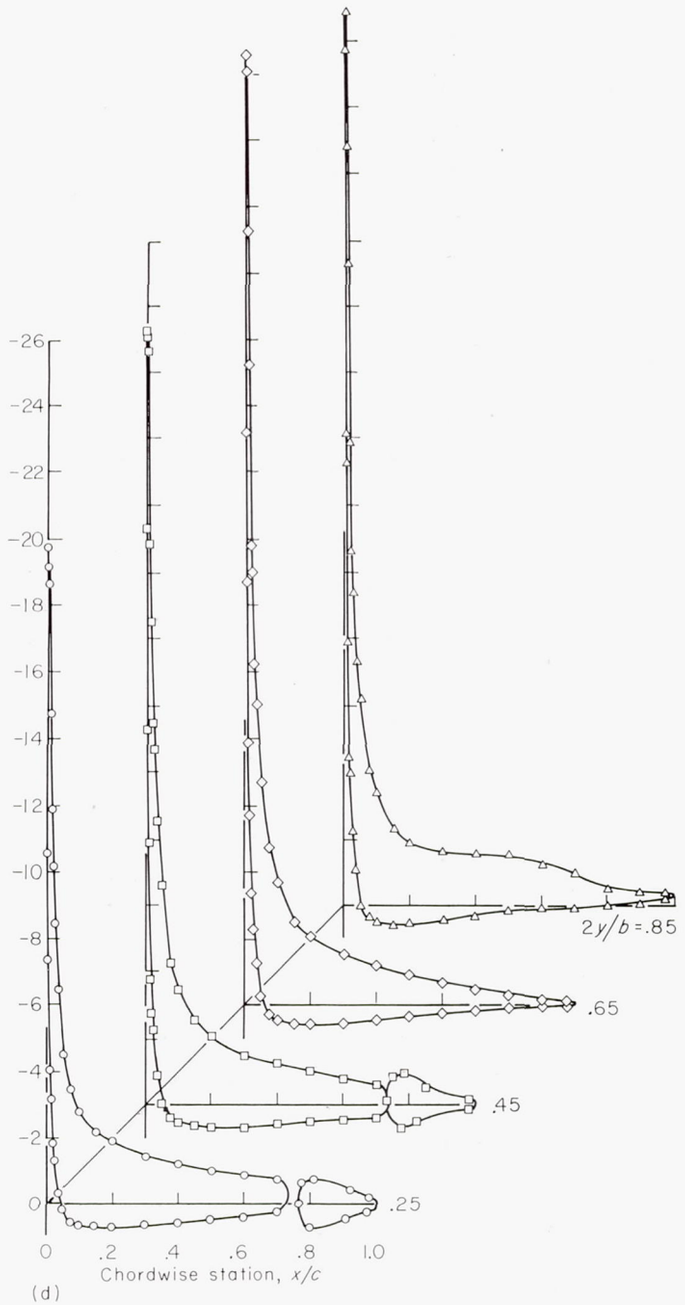


(d) $\alpha = 24.3°$

FIGURE 25.—Continued.

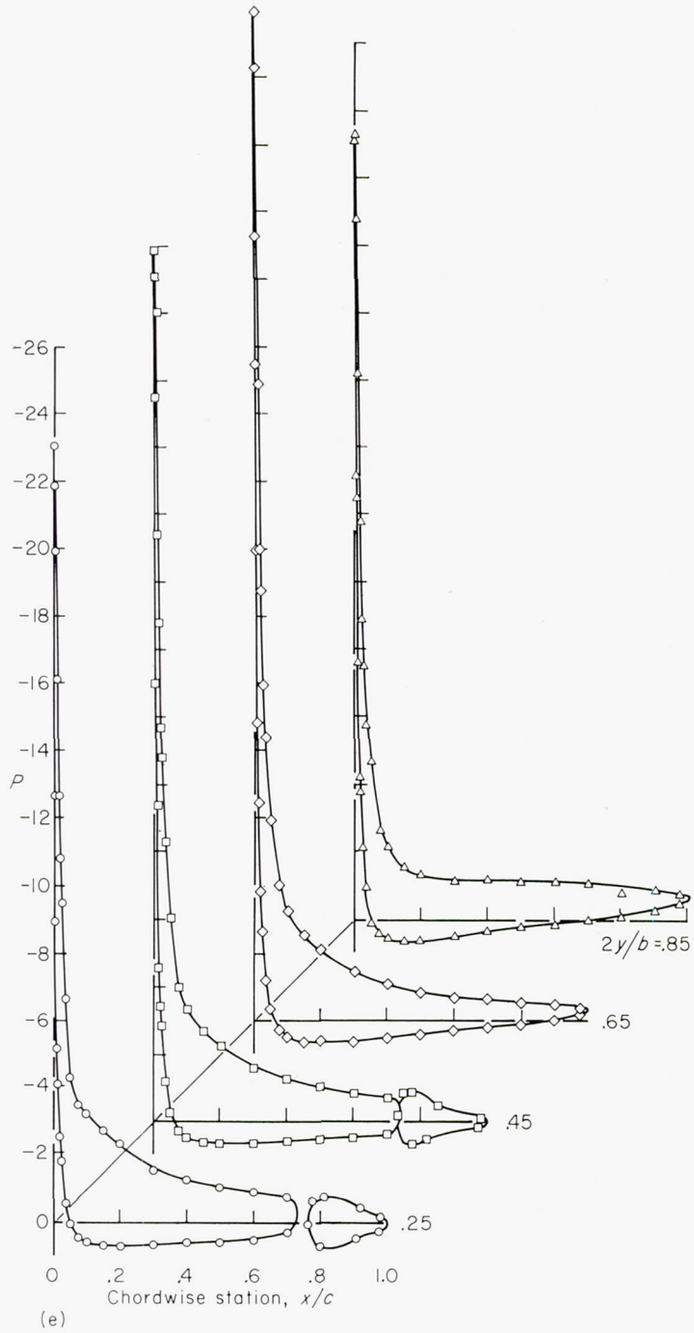


(e) $\alpha = 25.3°$

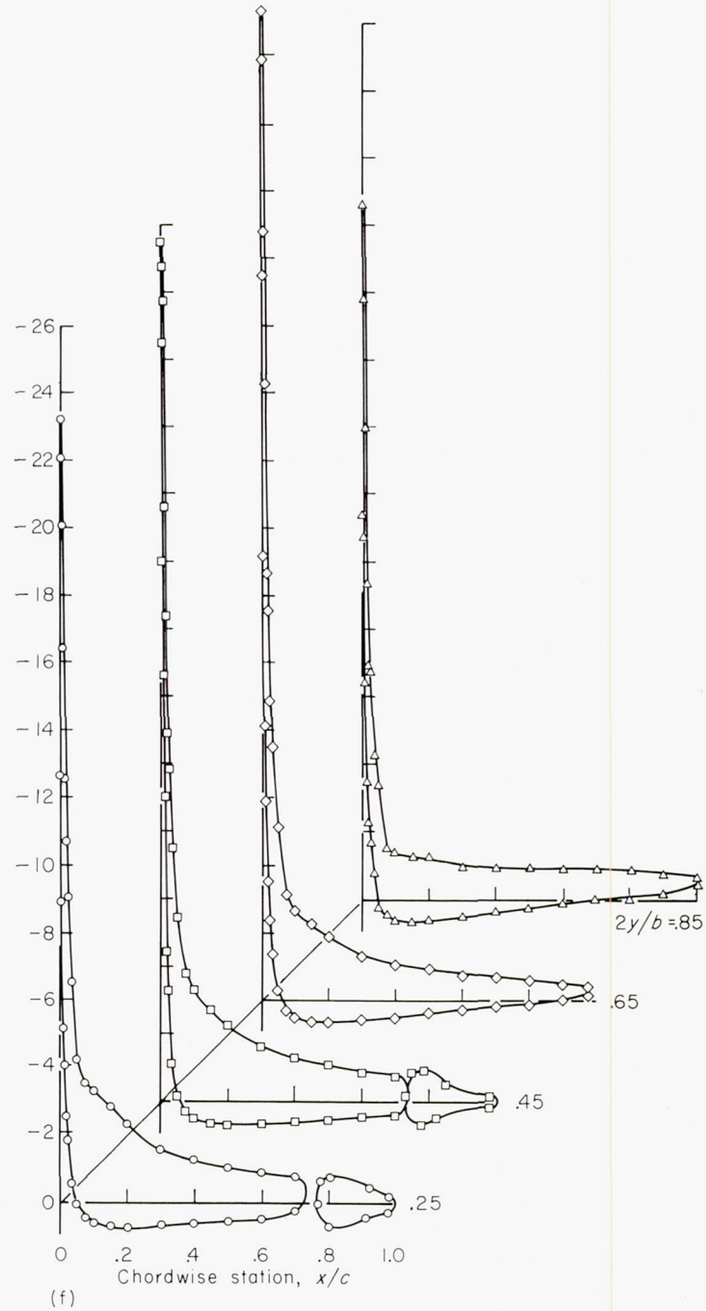


(f) $\alpha = 27.2°$

FIGURE 25.—Concluded.

U. S. GOVERNMENT PRINTING OFFICE: 1957